Generation of a

Human Induced Pluripotent Stem Cell Based Model of

Progerin Induced Aging

by

Sreedevi Raman

A Thesis Presented in Partial Fulfillment
of the Requirements for the Degree
Master of Science

Approved April 2017 by the
Graduate Supervisory Committee:

David Brafman, Chair
Sarah Stabenfeldt
Xiao Wang

ARIZONA STATE UNIVERSITY

May 2017

ABSTRACT

An *in vitro* model of Alzheimer's disease (AD) is required to study the poorly understood molecular mechanisms involved in the familial and sporadic forms of the disease. Animal models have previously proven to be useful in studying familial Alzheimer's disease (AD) by the introduction of AD related mutations in the animal genome and by the overexpression of AD related proteins. The genetics of sporadic Alzheimer's is however too complex to model in an animal model. More recently, AD human induced pluripotent stem cells (hiPSCs) have been used to study the disease in a dish. However, AD hiPSC derived neurons do not faithfully reflect all the molecular characteristics and phenotypes observed in the aged cells with neurodegenerative disease. The truncated form of nuclear protein Lamin-A, progerin, has been implicated in premature aging and is found in increasing concentrations as normal cells age. We hypothesized that by overexpressing progerin, we can cause cells to 'age' and display the neurodegenerative effects observed with aging in both diseased and normal cells. To answer this hypothesis, we first generated a retrovirus that allows for the overexpression of progerin in AD and non-demented control (NDC) hiPSC derived neural progenitor cells(NPCs). Subsequently, we generated a pure population of hNPCs that overexpress progerin and wild type lamin. Finally, we analyzed the presence of various age related phenotypes such as abnormal nuclear structure and the loss of nuclear lamina associated proteins to characterize 'aging' in these cells.

TABLE OF CONTENTS

CHAPTER Page

LIST OF TABLES

Table Page

LIST OF FIGURES

Figure Page

INTRODUCTION

1.1 Human Pluripotent Stem Cells

Tissue culture was developed in the early 1900s to study cellular response to normal and experimental conditions in a controlled environment. Since then, cell culture has evolved at a rapid pace allowing researchers to study individual cell phenotypes and genotypes to improve our understanding of human diseases and develop therapies to treat them. Primary cells derived from patients to study disease are generally terminally differentiated cells that do not expand indefinitely *in vitro*. Stem cells are characterized by their ability to self-renew and differentiate into specialized cell types. Based on their differentiation potential, stem cells can be multipotent (can differentiate into only a few cell types of the body), or pluripotent (can differentiate into all three germ layers) etc. In 1963, McCulloch and Till discovered the first human adult multipotent stem cells in the bone marrow, which regulate tissue homeostasis and damage repair in the body (Becker et al., 1963). However, these cells are rare, difficult to isolate and expand *in vitro*, and have a limited differentiation potential. Human embryonic stem cells (hESCs) and induced pluripotent stem cells (hiPSCs) are classified as human pluripotent stem cells (hPSCs), or a cell type that can differentiate into any cell type of the human body. hESCs are obtained from the inner cell mass of a human embryo and can propagate indefinitely under optimized cell culture conditions. As the extraction of the inner cell mass from the blastocyst destroyed the embryo, hESC culture was plagued with ethical controversies. hiPSCs resemble hESCs, but as they are generated by the overexpression of pluripotency factors in adult somatic cells, they provide an acceptable alternative to the controversial hESCs (Takahashi et al., 2007). As these cells can be derived from the somatic cells of a

diseased patient and then be differentiated into a specific cell type that demonstrates the diseased phenotype, these cells provide the most reliable in vitro snapshot of the mechanism (Soldner and Jaenisch, 2012). Human iPSCs led down the neuroectodermal lineage generate a population of multipotent stem cells called human neural progenitor cells (hNPCs), that are capable of indefinite expansion and have the potential to differentiate into various cell types of the central nervous system (Moya et al., 2014). These cells can be patterned to specific regions of the brain to yield a homogenous population of cells that can be differentiated into functional mature neurons with little to no tumorigenicity (Brafman, 2015).

1.2 Alzheimer's Disease

Alzheimer's disease (AD) is a progressive neurodegenerative age related disorder that has recently been shown to the third leading cause of death in the United States, after heart disease and cancer (James et al., 2014; Weuve et al., 2014). An early diagnosis for AD, the most common form of dementia is associated with increased survival time (Brookmeyer et al., 2011). A recent study indicates that the elimination of the AD pathology could reduce the prevalence of dementia by up to 50%, nearly 2.4 million cases by the year 2050 (Brookmeyer et al., 2016). The hallmarks of AD pathology include the aggregation of amyloid-beta (Aβ) plaques, neurofibrillary tangles of hyperphosphorylated tau protein, and neurodegeneration (Vickers et al., 2016). Although the exact mechanism of AD remains unclear, genetic mutations in the amyloid precursor protein (*APP*), Presenilin 1 (*PSEN1*), and Presenilin 2 (*PSEN2*) genes, that cause the early-onset familial AD (FAD) have been identified (Goate et al., 1991; St George-Hyslop et al., 1987; Sherrington et al., 1995; St George-Hyslop et al., 1992; Sherrington et al., 1996). A majority of the cases however are

the late-onset sporadic manifestation of AD (SAD), associated with various genetic and environmental risk factors. Apolipoprotein E (APOE) is one such genetic risk factor, the presence of an E4 allele of APOE is associated with an increased risk of developing AD (Kim et al., 2009). The presence of the more common E3 allele does not alter the risk of developing AD, whereas the E2 allele decreases the risk (Liu et al., 2013).

1.3 Alzheimer's disease modelling

AD models are crucial to understand the underlying disease mechanism and subsequently evaluate the efficacy of proposed therapeutics. *In vitro* iPSC-derived neurons from sporadic and familial Alzheimer's disease (SAD, FAD) patients are perhaps the most representative snapshot of the diseased state. Genetically modified knockout mice have been used to study the less prevalent familial form of the disease (Yang et al., 2000). A triple transgenic mouse model harboring *APP*, *PSEN* and Tau mutations was developed to study the interactions between Aβ and Tau and as well as their effects on the synapse (Oddo et al., 2003). However, owing to its genetic complexity, a model for the more common, late-onset sporadic form of AD is yet to be developed (Piaceri et al., 2013). With the discovery of the OSKM transcription factor cocktail to reprogram somatic cells into induced pluripotent stem cells(iPSCs), we are closer to patient specific disease models than ever before (Takahashi et al., 2007).

1.4 Stem cell reprogramming and age

The induction of pluripotency in adult somatic cells has been shown to reset the cellular age to a fetal state. Reprogrammed iPSCs demonstrate increased telomere length and mitochondrial fitness, closer to an embryonic stem cell, compared to their somatic parental cell (Marion et al., 2009). However, cellular hallmarks of aging such as shortened telomere

length, increased reactive oxidation species (ROS) in mitochondria, loss of heterochromatin, disruption in nuclear organization and increase in DNA damage etc. are not recapitulated upon terminal differentiation (Lapasset et al., 2011; Miller et al., 2013) . To model a progressive age-related neurodegenerative disorder such as Alzheimer's using patient derived iPS cells in vitro, it is critical to reintroduce the effects of aging (**Figure 1-2**). Aging cells using chemical stressors and toxins reintroduces phenotypes such as DNA damage and elevated ROS but fails to account for the protective mechanisms that these cells might use to counteract the same. Carbonyl-cyanide 3-chlorophenylhydrazone (3Cph; Sigma, C2759), a chemical stressor, is used in this study to induce the production of ROS in wildtype and transduced hNPCs to validate the increased production of ROS in aged cells.

1.5 Progerin induced aging

Hutchinson-Gilford progeria syndrome (HGPS) is a disease characterized by accelerated premature aging, most commonly due to a point mutation in the gene encoding the nuclear envelope protein lamin (Scaffidi and Misteli, 2006). The silent point mutation activates a cryptic splice site in exon 11 of *LMNA* generating a progerin mutant with a deletion of 150 nucleotides (**Figure 1-3**). In a normal cell, the farnesylation of the wild type lamin protein allows for its localization to the nuclear envelope, after which the farnesyl group is cleaved. The 50-amino acid deletion in the progerin mutant protein however leads to a loss in the cleavage site of the farnesyl group, and it remains attached to the mature protein on the nuclear envelope (Capell et al., 2007). The expression of mutant progerin is associated with abnormalities in nuclear morphology and function, including the downregulation of nuclear proteins like LAP2a, HP1γ, RANBP17 (Mertens

et al., 2015; Scaffidi and Misteli, 2005). Struder et al. demonstrate that the ectopic expression of progerin in neurons derived from iPSCs of a Parkinson's patient restores the hallmarks of aging in the cell (Miller et al., 2013). We propose to examine the effects of overexpressing progerin in AD patient derived NPCs on cellular age.

1.6 Gene delivery

Researchers use gene delivery to introduce exogenous genetic information or to edit endogenous genes to generate iPSCs, induce their differentiation, or to recapitulate diseased phenotypes in patient-derived cells (Nayerossadat et al., 2012). Genetic elements can be delivered to cells using viral or non-viral methods that can result in the integration of the gene, or its transient expression in the cell. Retroviruses are RNA viruses that infect dividing cells and allow for stable integration at random insertion sites in DNA. An outer lipid envelope containing viral glycoproteins encapsulates two copies of positive sense RNA (**Figure 1-4**). After the viral glycoproteins recognize and bind to cell surface receptors, the virus fuses with the membrane and is endocytosed to release the contents into the cytoplasm (**Figure1-4**). The viral RNA is then reverse transcribed by a viral reverse transcriptase enzyme in the cytoplasm of the cell and the resulting DNA is translocated to the nucleus of the cell during mitosis (Coffin, 1992). In our system, the viral transfer vector is driven by the SV40 promoter and includes a green fluorescent protein (GFP) tag and a puromycin cassette to allow for the selection of transduced cells. (**Figure1-5, A**). A retrovirus to deliver the transfer plasmid can be generated by the co-transfection of a packaging cell line, such as the HEK 293Ts, with viral plasmids (packaging, envelope and transgene of interest) (**Figure1-5, B**).

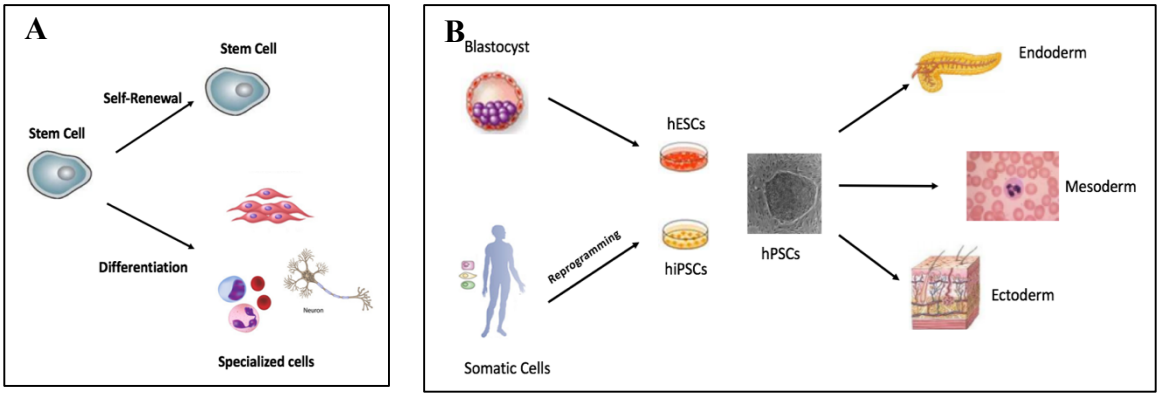

Figure 1-1: **Human Pluripotent Stem Cells**

Stem cells are characterized by the ability to self-renew and differentiate into specialized cell types (**A**). Stem cells derived from the inner cell mass of the blastocyst and reprogrammed from adult somatic cells are classified as human pluripotent stem cells (hPSCs) that can differentiate into cell types of all three germ layers (**B**).

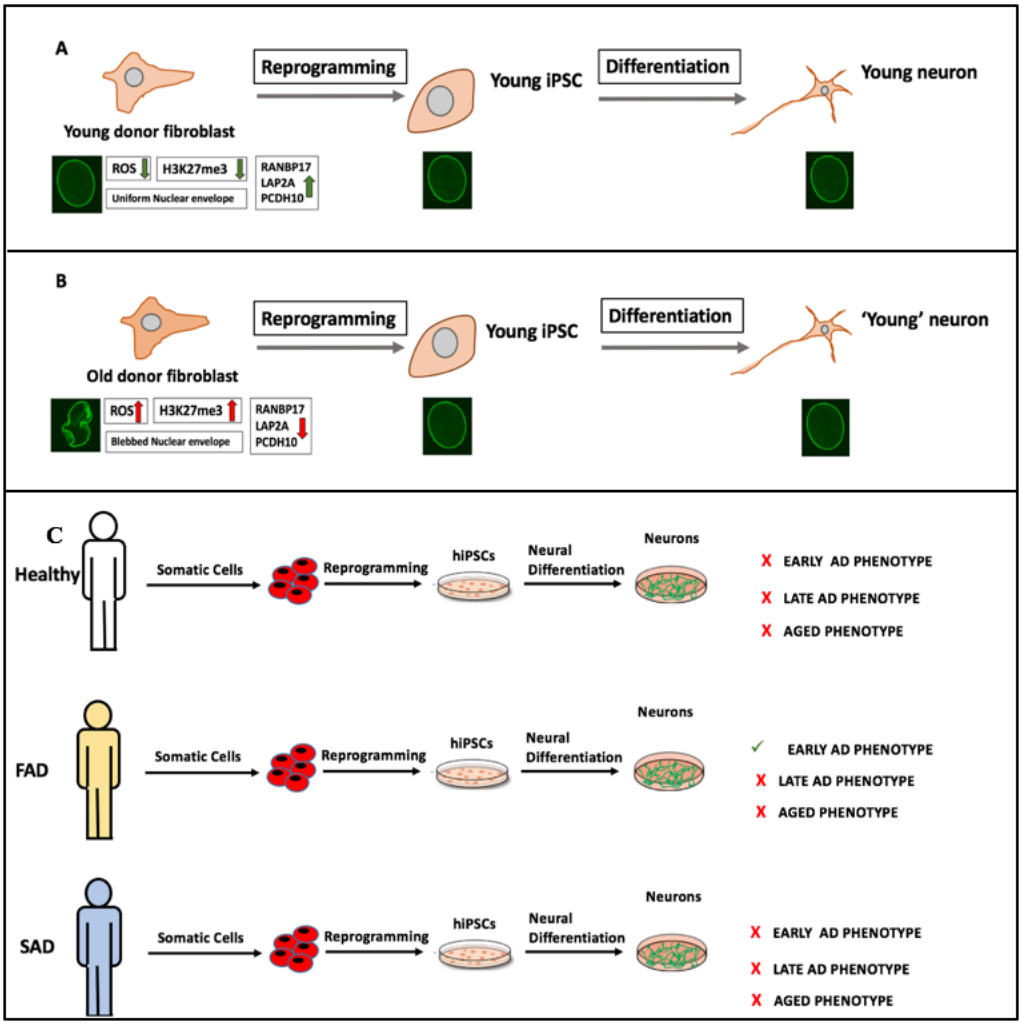

Figure 1-2: **hPSC reprogramming and disease modelling**

Hallmarks of aging are observed to be reversed upon reprogramming(**A-B**). For example, nuclear morphology is uniform, mitochondrial function is restored, telomeres are lengthened, DNA damage is reduced and structural proteins (RANBP17, LAP2A, PCDH10 etc.) are upregulated to restore nuclear organization. Currently available hPSC models of Alzheimer's disease do not recapitulate all early and late phenotypes that manifest in familial AD (FAD) and sporadic AD (SAD) (**C**).

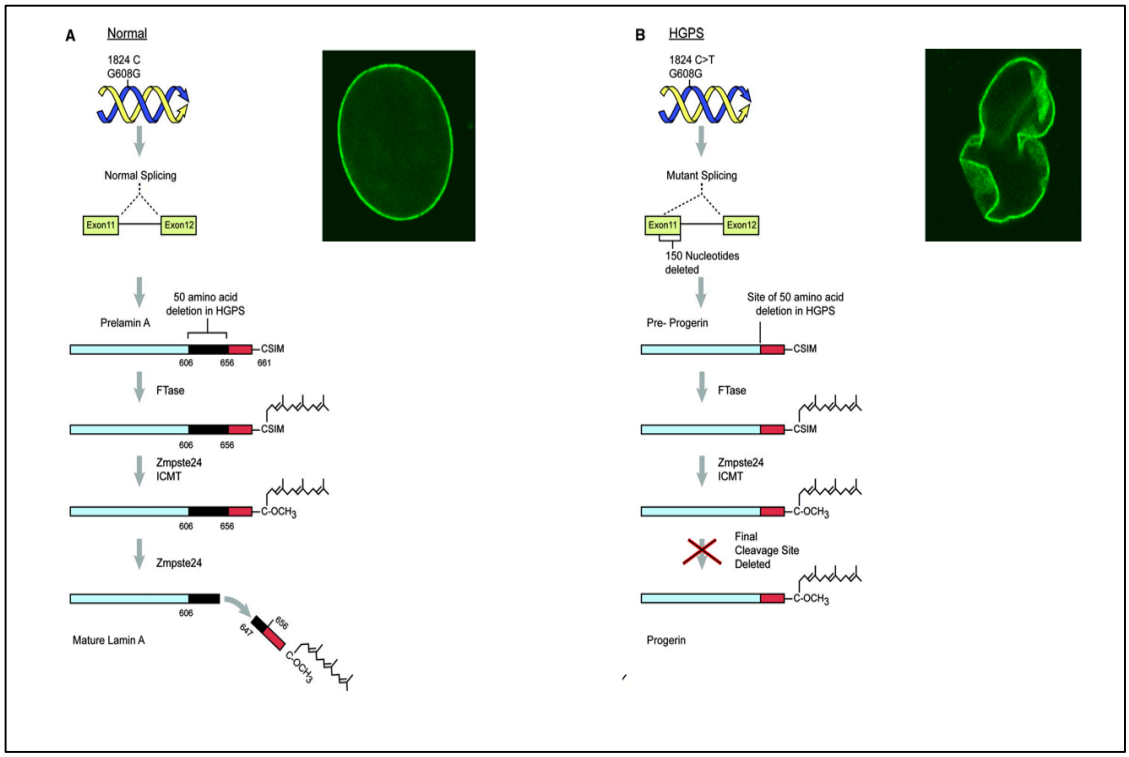

Figure 1-3: Mutant Lamin-A processing in HGPS patients

A silent mutation in *LMNA* gene leads to the activation of a cryptic splice site causing the aberrant processing and mutant splicing of the lamin transcript. A 150 nucleotide deletion in the transcript due to mutant splicing generates the progerin protein that lacks a cleavage site for the farnesyl group (Capell et al., 2007).

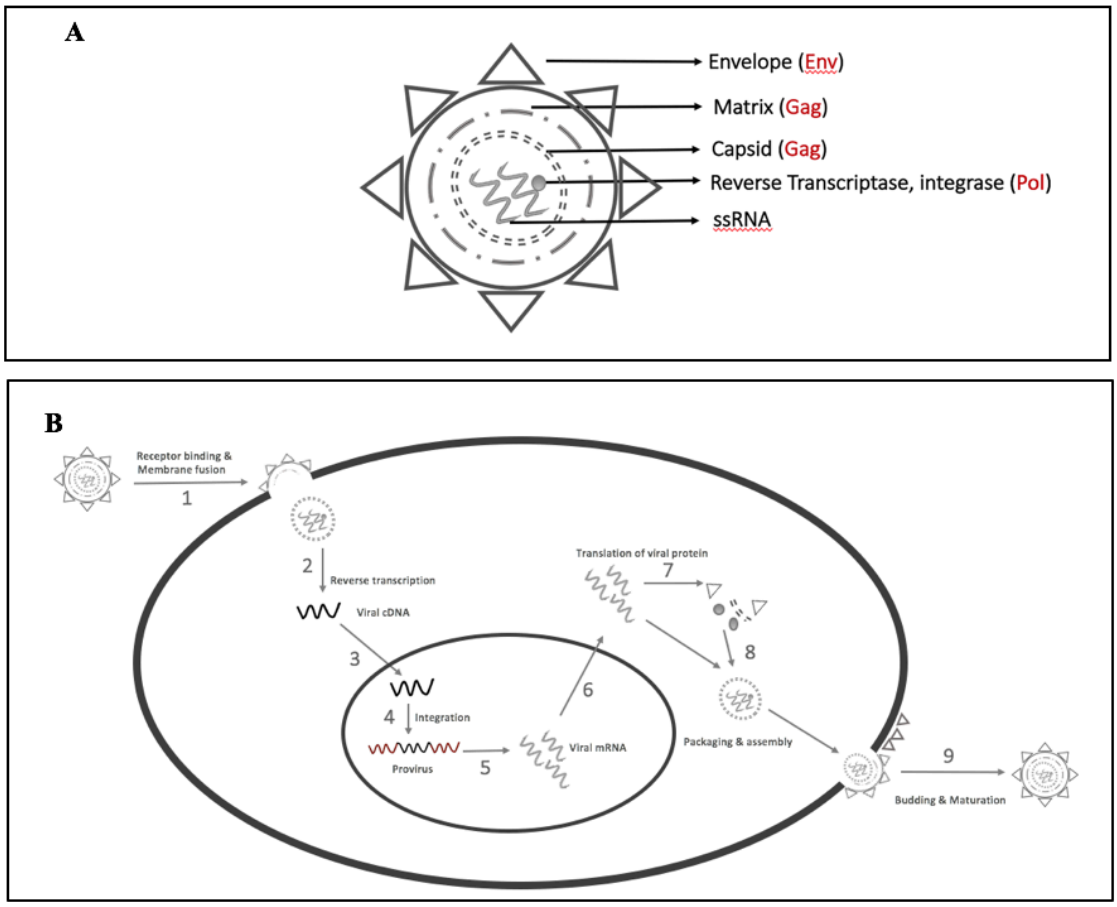

Figure 1-4: The structure and replication cycle of a viral particle.

Based on viral tropism, the envelope of the virus is recognized by cell surface receptors leading to membrane fusion. Once inside the cytoplasm, the reverse transcription of viral RNA produces complementary DNA (cDNA) molecules that then translocate to the nucleus. This is followed by the integration of the viral cDNA into the host genome, generating the provirus. Viral mRNA is then transcribed within the nucleus, and subsequently the host cell machinery translates viral protein in the cytoplasm, including the expression of envelope proteins on the cell membrane. Following the packaging and assembly of a viral particle, it matures upon exit from the host cell by budding. (Figure adapted from Fanales-Belasio et al.,2010)

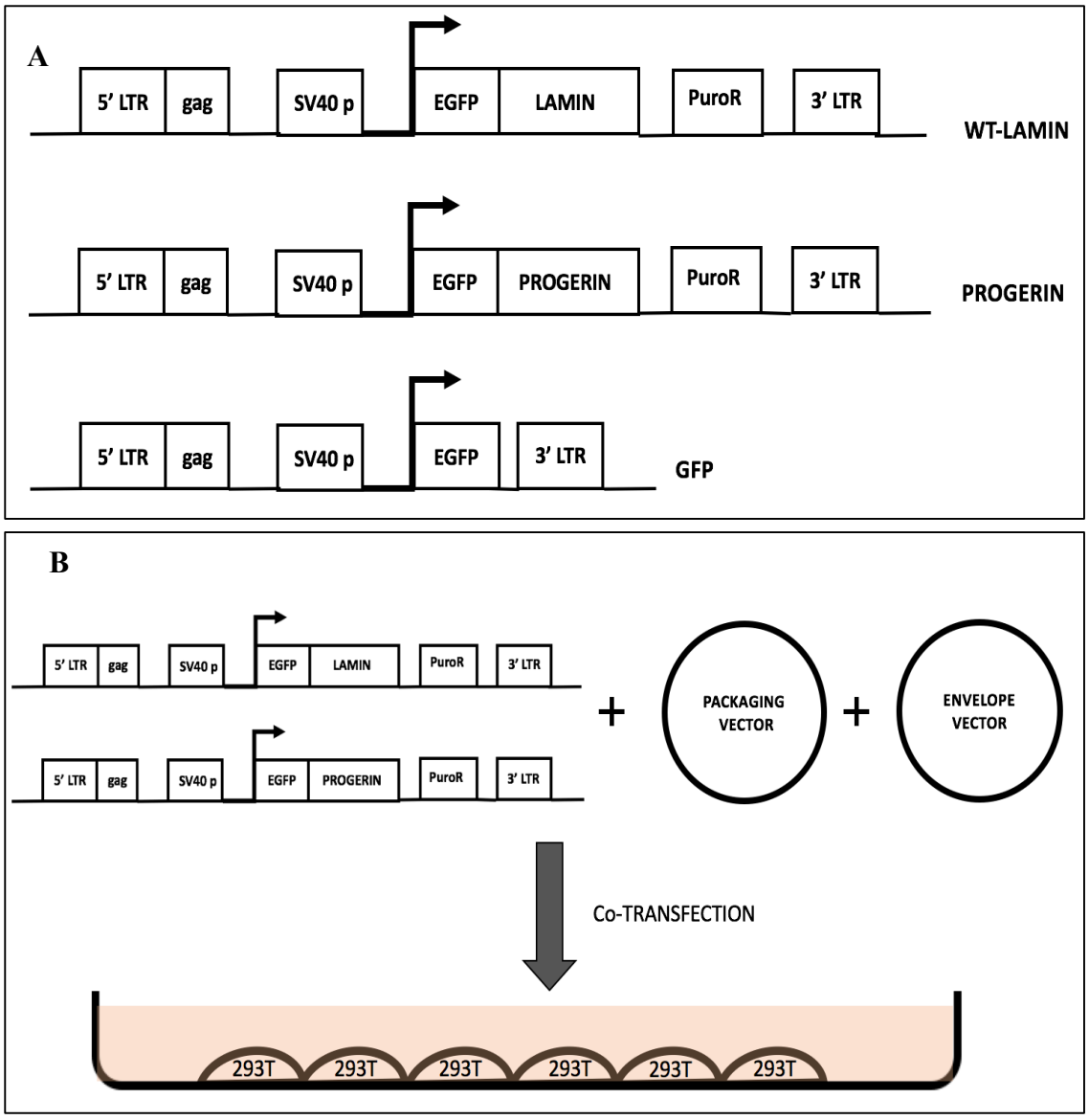

Figure 1-5: Viral vector to overexpress transgene

The viral LTR flanks the wt-lamin/progerin/GFP only transgene (**A**). The SV40 promoter drives the expression of the GFP tagged nuclear proteins and a puromycin cassette that allows for the selection of transduced cells. The co-transfection of the viral proteins in a packaging cell line generates virus (**B**).

2. MATERIALS AND METHODS

2.1 Cell Culture

All reagents used to prepare media were obtained from Life Technologies unless otherwise mentioned. Human Embryonic Kidney 293T cells were cultured on poly-L-ornithine (PLO) coated substrates. PLO plates were prepared by adding 10 μg/mL PLO (Sigma, P3655) to tissue culture treated plates and incubating at 37°C for 4 hours (h). The PLO solution was then aspirated and the plates were washed twice with DPBS before seeding cells supplemented in 293T media (DMEM, 10% FBS, 1% Pen/Strep).

Human neural progenitor cells (hNPCs) were cultured on PLO-Laminin (LN) coated substrates. The method to coat these plates is as follows: PLO coated tissue culture plates were washed thrice with PBS and then coated with mouse LN (5 ug/mL) diluted in cold PBS. The plates were incubated for 4h at 37°C after which they were sealed with parafilm and stored at -20°C till use. The plates were washed twice with PBS before seeding cells suspended in neural expansion media (1X DMEM-F12, 1% (v/v) N2 supplement, 1% (v/v) B27 supplement, 1% (v/v) Glutamax, 1% (v/v) Pen/Strep) supplemented with 30ng/mL mouse FGF2 (Peprotech) and 30 ng/ml mouse EGF (Life Technologies). During the passage of hNPCs, 5 uM Rho kinase inhibitor (Y-27632) was used to promote single cell survival. Freeze backs of cells were aliquoted in cryogenic vials (VWR, 10018-738) in freezing media containing 90% FBS, 10% DMSO (Sigma, D2650) and stored at -80°C in Mr. Frosty freezing containers for 24h before transferring to -150°C.

2.2 Plasmid cloning and purification

Bacterial stabs of the transfer vectors (Addgene # 17662, 17663, 10668), packaging vector (Addgene # 8449), and envelope vector (Addgene # 8454) were used to streak appropriate antibiotic resistant agar plates (**Appendix C**). The plates were incubated at 37 °C for 12 hours after which single colonies were picked to inoculate 3 mL Millers LB media (Sigma, I8388) containing antibiotic. After 14 hours of growth at 37°C on a shaker at 225rpm, plasmids were extracted from 1 mL culture using Miniprep Kits (Qiagen, 27106). The identity of each plasmid was verified on a 1% agarose gel after a double-restriction-digest reaction using enzymes purchased from ThermoFisher. The verified plasmids were then grown up in a larger liquid culture (250mL) containing antibiotic. A DNA extraction kit (Macherey-Nagel, 74014) was used to extract high concentrations of plasmid DNA (>1 μg/uL). The plasmids were stored at -20 °C and thawed on ice before use.

2.3 Transfection of HEK 293T

2.3.1 Electroporation

Healthy low passage HEK 293T cells were dissociated from 80% confluent 10 cm plates using accutase. The dissociation enzyme was neutralized by the addition of an equal volume of DMEM and cells were pelleted by centrifugation at 200g. The cells were resuspended in 293T media (DMEM,10% FBS, 1% Pen/Strep) for counting. Tubes were set up with $5x10^6$ cells per electroporation reaction and the cells were washed with 1x DPBS to remove traces of serum. The cells were resuspended in 100uL of buffer R of the 100 μL neon transfection kit. The packaging (Addgene, 8454), envelope (Addgene, 8449) and transfer plasmid constructs (Addgene 17662, 17663)

were added to a sterile Eppendorf tube with 25µg total DNA per electroporation reaction (12.5µg x DNA, 8.25µg UMVC, 4.25µg VSVG). The DNA and cells were mixed by gently flicking the tube and cell-DNA mixture was electroporated using the 100µL gold Neon tip at 1100V for 2 pulses of 20ms (ThermoFisher, MPK10025). The transfected cells were transferred to a PLO coated 10cm plate containing 10mL of antibiotic free 293T media. At 24 hours, the media was switched to 293T media with antibiotic. Viral conditioned media was collected from 4x 10cm plates at 48 and 72 hours post transfection.

2.3.2 PEI Transfection

Healthy low passage HEK 293T cells were dissociated from 80% confluent 10 cm plates. The dissociation enzyme was neutralized by the addition of an equal volume of DMEM and cells were pelleted by centrifugation at 200g. The cells were resuspended in 293T media (DMEM,10% FBS, 1% Pen/Strep) and seeded at $5x10^6$ to ensure 60-70% confluency on day 1. On the day of transfection, the media on the plate was changed to 293T cell culture media without antibiotic (DMEM, 10% v/v FBS). The packaging (Addgene, 8454), envelope (Addgene, 8449) and transfer plasmid constructs (Addgene 17662, 17663) were added to a sterile conical with 18µg total DNA per reaction (12.5µg x DNA, 8.25µg UMVC, 4.25µg VSVG). The DNA was diluted in DMEM and recommended volume of the polyethylinimine (PEI) reagent (PolySciences, 23966-2). After incubating for 15 minutes, the DNA-polymer complexes were added to the HEK293T cells. The media was changed 6h post transfection and conditioned cell supernatant was collected at 24 and 52 hours.

2.4 Concentration of virus

The conditioned media was centrifuged for 5 minutes at 400g to remove any cell debris from suspension. It was then filtered through a 0.45 um cellulose acetate filter, after which 10mL of LentiX concentrator (ClonTech, 631231) was added to 30mL of filtered conditioned media. The tube was inverted a few times to mix and incubated at 4°C for 40 minutes. The virus was pelleted by centrifugation at 1500g for 45 minutes at 4°C. The viral pellet was gently resuspended in cold DMEM while ensuring no bubbles were introduced.

2.5 Transduction of hNPCs

Human neural progenitor cells were transduced with concentrated virus when they were 40% confluent on a 6 well PLO/Ln coated tissue culture plate. Transduction efficiency was enhanced by the addition of 8 ug/mL of polybrene (Sigma, H9268-5G). The media was changed 24 hours post infection and transduction efficiency was evaluated 72 hours post infection using flow cytometry. The cells were passaged to a 12 well plate and antibiotic selection was started when cells were 80% confluent using 200ng/mL puromycin (Life Technologies, A11138-03).

2.6 Flow cytometry

Cells were dissociated in Accutase (Life Technologies, A1110501) for 5 min at 37°C and broken up into single cells. The cells were then washed and resuspended in stain buffer (BD Biosciences, 554656) maintaining the cell count at < 1000 events/uL of buffer. Cells were analyzed on a FACSCanto (BD Biosciences) or ACCURI C6 (BD Biosciences). For GFP positive live cells, the FL1 channel was used to measure fluorescence intensity after gating appropriate non-fluorescent controls for forward and

side scatter. To stain for histone methylation mark H3K27me3, cells were fixed for 30 min on ice with BD Cytofix Fixation Buffer (BD Biosciences). After washing twice with stain buffer, the cells were permeabilized for 30 min on ice using BD Phosflow Perm Buffer III (BD Biosciences). Cells were then washed twice with stain buffer and one test volume of antibody (EMDMillipore, 07-499) was added for each 100 uL of cell suspension. Cells were incubated at 37°C for 30 min after which they were washed, and resuspended in stain buffer containing the secondary antibody for 30 min. The stained cells were then washed twice before flow cytometry analysis (gated with a 2° antibody only control). For measuring ROS, cells were incubated with MitoSOX™ Red (ThermoFisher, M36008; 5uM diluted in media) for 10 minutes at 37°C and resuspended in stain buffer. To induce stress, cells were treated with 3Cph (3.5uM) for 48h prior to ROS quantification using flow cytometry.

2.7 RNA Isolation from Brain samples

Cortical brain samples from patients with no prior neurological diagnoses were obtained from sources listed in Appendix A. Samples were sliced into small sections using a sterile blade and forceps on a petridish placed on dry ice. The sections were collected in a microhomogenizer Eppendorf tube (Clontech, 9791A) and 800uL of cold TRIzol (ThermoFisher, 15596018) was added to homogenize the sample. The homogenized sample was placed at 65°C for 5 min and 200µL of chloroform was added to the sample while still warm. The sample was mixed by vigorous shaking for 30 seconds after which it was placed on ice for 5 minutes. Following centrifugation at 1000 rpm for 5 min the aqueous phase was transferred to a new tube. One volume of

70% ethanol was added to the sample and the RNA was then purified using the NucleoSpin RNA Kit (Macherey-Nagel, 740955).

2.8 Quantitative PCR (qPCR)

RNA was isolated from biological samples using the NucleoSpin RNA Kit (Macherey-Nagel, 740955). Reverse transcription of 1000ng of RNA was performed with the iScript RT Supermix (Bio-Rad). Quantitative PCR was run using the iTaq Universal SYBR Green Supermix (Bio-Rad) on a CFX384 TouchTM Real-Time PCR Detection System. A 2 min gradient to 95°C was followed by 40 cycles at 95°C for 5 s and 60°C for 30 s. Primer sequences used in the assay are detailed in Appendix B. Gene expression was normalized to 18S rRNA levels. Delta Ct values were calculated as C_{target}-Ct_{18s}. The $2^{-\Delta\Delta Ct}$ method was used to analyze raw data and calculate relative fold changes in gene expression (VanGuilder et al., 2008).

2. 9 Immunofluorescence

Prior to fixation, cells were washed twice with stain buffer (BD Bio- sciences). The cells were then fixed for 30 min at room temperature (RT) with BD Cytofix Fixation Buffer (BD Bio- sciences). After two washes with the staining buffer, the cells were permeabilized with BD Phosflow Perm Buffer III(BD Biosciences) for 30 min at 4°C. The cells were washed twice with stain buffer before incubating at 4°C overnight with the primary antibody for NESTIN. Following two washes with stain buffer the cells were incubated with secondary antibodies at RT for 1 h. DNA was stained with Hoechst 33342 (2 μg/ml; Life Technologies) for 10 min at RT and then washed twice with stain buffer. Stained cells were imaged using an EVOS microscope (Life Technologies).

3. RESULTS

3.1 OPTIMIZATION OF VIRUS PRODUCTION IN HEK 293T CELLS

The vector map of the plasmids containing the wild type and mutant *LMNA* gene is described in **Figure 1-4**. The simian virus 40 (SV40) promoter drives the expression of the nuclear envelope protein tagged with a green fluorescent protein(GFP) reporter. The plasmid also contains a puromycin resistance cassette that allows for the antibiotic selection of transfected mammalian cells. The complete plasmid maps presented in **Appendix -C** contain the restriction enzyme sites that were used to verify the identity of the constructs using a double digest.

3.1.1 Electroporation increased viral plasmid transfection efficiency in HEK293Ts

The efficient delivery of viral plasmids to the HEK293T packaging cell line is critical to generate functional viral particles. The transient transfection of the 293T cells allows for the generation of viral particles that subsequently infect cells with virus encoding the GFP-expressing transgene. Thus, the transfection efficiency is an indicator of the titer of the virus in the cell supernatant. We compared the efficiency of gene delivery by electroporation with chemical transfection using polyethylenimine (PEI). Source plates transfected using electroporation displayed a higher transfection efficiency compared to PEI transfected HEK293Ts (**Figure 3-1**). The higher transfection efficiency of the GFP-only source plates can be attributed to the smaller size of the transgene.

3.1.2 Lamin/Progerin overexpression verified in 293T cells using qRT-PCR

The activation of the cryptic splice site due to a point mutation in the lamin-A gene leads to the deletion of a 150 nucleotide deletion in the transcript, generating the progerin

protein (Eriksson et al., 2003). Primer pairs spanning across the splice site consensus sequence were used to verify the expression of full length wild type lamin (wt-lamin) and truncated (mutant) progerin (Scaffidi and Misteli, 2006). The 'lam full' primer pair spans from exon 9 through exon 11, across the consensus splice sequence. In lamin transfected cells, a 511 bp product is expected upon PCR amplification. However, in cells overexpressing progerin, a 150 bp deletion causes the expression of a truncated 361 bp product. The 'prog mut' primer pair detects part of exon 11- exon 12 that is discontinuous in wt-lamin, but yields an 87 bp product in progerin overexpressing cells. The overexpression of full length lamin/truncated progerin in infected HEK293Ts was confirmed by qRT-PCR. The products were run on a 4% agarose gel to improve band separation, as described in **Figure 3-2**.

3.2 OPTIMIZATION OF VIRAL TRANSDUCTION IN HUMAN NEURAL PROGENITOR CELLS (hNPCs)

The stable integration of a transgene into the genome of a target cell can be achieved through retroviral transduction. The efficiency of viral transduction is dependent on the titer of functional viral particles infecting a cell. To generate virus, retroviral envelope and packaging plasmids are co-transfected with the transgene of interest into a packaging cell line like human embryonic kidney (HEK) 293T cells (Louis et al., 1997) (**Figure 1-5**). The HEK 293T cells are transformed with ~4.5kb of the adenoviral genome and can be used for the propagation of viral vectors. These cells are easily transfected and express the large T-antigen that binds to the SV40 promoter region of viral vectors and allows for the episomal replication and expression of the transfer plasmids. The 293T cells produce and

package viral components that mature as they bud out of the cell with host membrane, that now expresses viral envelope proteins. The cell supernatant of transfected 293Ts contains mature viral particles that proceed to infect other cells in order to propagate the viral cell cycle. The transfer plasmids are designed to be replication incompetent, or self-inactivating, to address safety concerns involved in working with infectious viral particles. Self-inactivating vectors contain a deletion in their 3'long terminal repeat (LTR) promoter that is copied into the 5'LTR in viral progeny. This deletion prevents the replication in an infected cell, halting the propagation of the viral life cycle (Zufferey et al., 1998). As the wt-lamin and progerin constructs contain the GFP fluorescence reporter, the transduction efficiency of the hNPCs was quantified using flow cytometry and considered representative of the viral titer.

3.2.1 Chemical concentration improves viral transduction efficiency

The titer of virus in the harvested cell supernatant is dependent on a multitude of factors, including the health of the packaging cell line, the transfection efficiency, the transgene itself, and the method of storage (Tiscornia et al., 2006). The multiplicity of infection (MOI), or the average number of viral particles infecting each cell, can be increased by concentrating viral particles from larger volumes of cell supernatant. Viral pellets can be resuspended in small volumes following high speed centrifugation in an ultracentrifuge (70,000g). As this specialized centrifuge was not readily accessible to us, we used a commercially available concentrating reagent. Virus can also be concentrated by adding chemical reagents to the cell supernatant that precipitate viral particles upon centrifugation at relatively low speeds (1,500g). Precipitation of the virus with the LentiX

chemical concentrator increased the viral titer, leading to ~15-fold increase in transduction efficiency (**Figure 3-3**).

3.2.2 Polybrene induces increase in transduction efficiency

Cationic lipopolymers like polybrene (hexadimethrine bromide) have been shown to increase retroviral transduction efficiency by reducing the electrostatic repulsive forces between a negatively charged cell and the negatively charged viral envelope (Davis et al., 2002; Denning et al., 2013). Flow cytometry was used to quantify GFP as a measure of transduction efficiency both in the presence and absence of polybrene (**Figure 3-4)**. The transduction of hNPCs with LentiX-concentrated GFP, Lam-GFP and Prog-GFP virus showed a marked increase in the presence of polybrene (8ug/mL). The higher increase in GFP-only virus transduction efficiency could be attributed to the relatively small size of transgene to be packaged.

3.2.3 Antibiotic selection enriches for transduced hNPCs

As transduction of hNPCs with the Lamin/Progerin-GFP virus conferred puromycin resistance to infected cells, the transduced cell population could be enriched using antibiotic selection. Following a kill curve to identify the optimal concentration of puromycin for selection, the cells were routinely passaged in the presence of antibiotic (0.2ug/mL). In the absence of antibiotic selection, the uninfected population of GFP-negative cells stabilized. Cells passaged in puromycin were more than 40-fold enriched for the transduced GFP-positive population (**Figure 3-5, A**). Fluorescence activated cell sorting (FACs) was used to further isolate a pure population as the ratio of the transduced to non-transduced cells decreased with passaging post infection (**Figure 3-5, B**).

3.3 VALIDATION OF SELECTED hNPCs

3.3.1 Confirming Lamin/Progerin expression in hNPCs using qRT-PCR

The transduction of hNPCs with wild type lamin and progerin retrovirus leads to the stable expression of the nuclear envelope protein due to the genomic integration of the transgene. The expression of full length lamin (wt-lamin) and truncated lamin (progerin) was confirmed by qRT-PCR with the 'lam full' primer spanning the consensus splice sequence (**Figure 3-6, A**). The amplified products were run on a 4% agarose gel to improve band separation and detection of the 87 bp mutation specific sequence that is absent in Lamin-GFP hNPCs (**Figure 3-6, A**). The expression of progerin was ~1000 fold elevated in Progerin-GFP hNPCs compared to its expression in Lamin-GFP hNPC population (**Figure 3-6, B**).

3.4 ASSAYS FOR AGING MARKERS IN hNPCs

3.4.1 Progerin overexpression causes blebbing of nuclear envelope

The identity of the transduced hNPCs was confirmed by immunostaining for the neurofilament marker NESTIN, that is expressed by neural stem/progenitor cells (Suzuki et al., 2010) (**Figure 3-7, C-H**). The mixed population of non-transduced wt hNPCs and Lamin-GFP/Progerin-GFP hNPCs expressed NESTIN. Progerin overexpressing cells display a non-uniform blebbed nuclear envelope **(**Scaffidi et al.,2005). The GFP tagged nucleus of wt-lamin expressing Lamin-GFP NPCs exhibit a uniform morphology (**Figure 3-7, A**), whereas the progerin expressing Progerin-GFP hNPC nuclei display folding and blebbing of the nuclear envelope (**Figure 3-7, B).**

3.4.2 Progerin expressing hNPCs have higher levels of mitochondrial ROS

Flow cytometry was used to quantify the mitochondrial reactive oxidation species (ROS) in Lamin/Progerin-GFP hNPCs. Carbonyl-cyanide 3-chlorophenylhydrazone induced stress was used as a positive control to measure elevated ROS in Lamin/Progerin-GFP hNPCs (**Figure 3-8**, **B**), with unstained hNPCs as the threshold for red fluorescent protein(RFP) signal (**Figure 3-8**, **A**). In the absence of the 3Cph, Progerin-GFP cells exhibit higher ROS than Lamin-GFP hNPCs (**Figure 3-8**, **C**).

3.4.3 Elevated levels of repressive histone methylation marks in progerin expressing hNPCs

Elevated levels of the repressive histone mark H3K27me3 have been observed in tissue from an adult mouse brain (Tang et al., 2014). We measured the level of the repressive histone mark in transduced lamin and progerin hNPCs using immunostaining for the H3K27me3 mark followed by flow cytometry analysis (**Figure 3-9**). The progerin overexpressing hNPCs exhibit a higher level of the histone mark compared to the wild type lamin expressing hNPCs.

3.4.4 Tau 4R isoform absent in transduced hNPCs

The Tau 3R/4R mRNA isoform ratio has been demonstrated to be about 1:1 in a normal adult human brain (Iovino et al., 2010). The expression of the 3R and 4R Tau isoforms was quantified in the Lamin/Progerin-GFP hNPCs using qRT-PCR. The amplified RT-PCR products were run on a 2% agarose gel to separate the two Tau isoforms. The adult brain sample showed 3R and 4R Tau expression, whereas the fetal brain and hNPC samples expressed the only the 3R isoform (**Figure 3-10**).

3.4.5 Progerin transduced hNPCs exhibit Lamin-GFP hNPC like expression levels of genes downregulated during aging

Gene expression analysis of aged cells has revealed the downregulation of various genes involved in nuclear transport and cellular function (Mertens et al., 2015; Vidak et al., 2015). This was confirmed by examining the expression levels of these candidate genes in cortical samples from the human adult brain (16 - 93 years). Following RNA isolation from fetal and adult brain tissue, cDNA was synthesized for qRT-PCR analysis to measure age related gene expression levels **(Figure 3-11, A)**. The adult brain samples displayed the significant downregulation of 5 aging genes (*CACNG4,FBN3,HP1γ,NKAIN2,PCDH10*) compared to the fetal brain **(Figure 3-11, B)**. There was no significant difference in the expression levels of these genes in the Progerin-GFP hNPCs relative to the wt-lamin expressing hNPCs **(Figure 3-11, C)**. RNA sequencing (RNA-Seq) analysis indicated the significant upregulation of 64 genes and significant downregulation of 102 genes in Progerin-GFP hNPCs compared to the Lamin-GFP and wt hNPCs **(Figure 3-12).** The candidate aging genes considered in **Figure 3-11** however were not part of this differentially expressed subset.

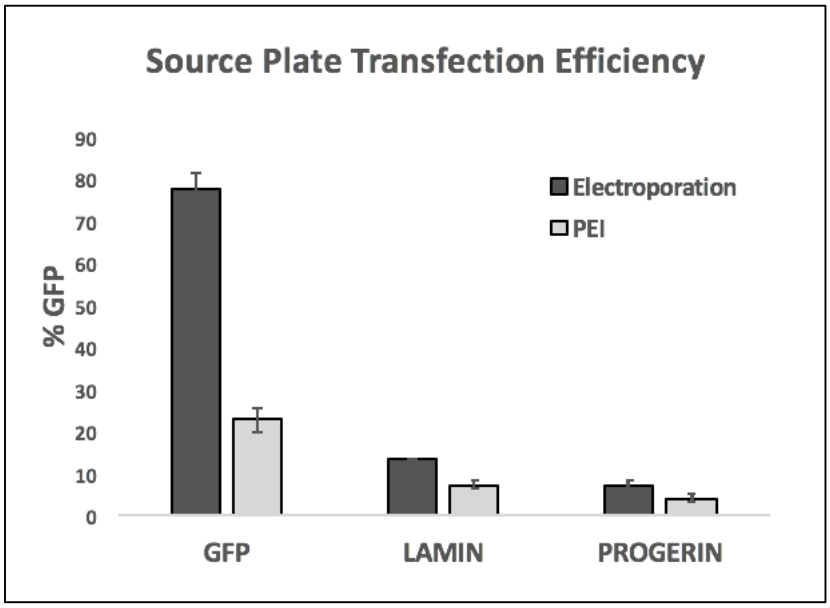

Figure 3-1: Electroporation increased viral plasmid transfection efficiency in HEK293T compared to chemical transfection methods

Flow cytometry data of HEK293T cells transfected with envelope, packaging and transfer (GFP, Lamin, Progerin) viral plasmids. The transfection efficiency, quantified by the number of GFP positive cells, was larger in the case of electroporation mediated gene delivery relative to the chemical transfection using PEI.

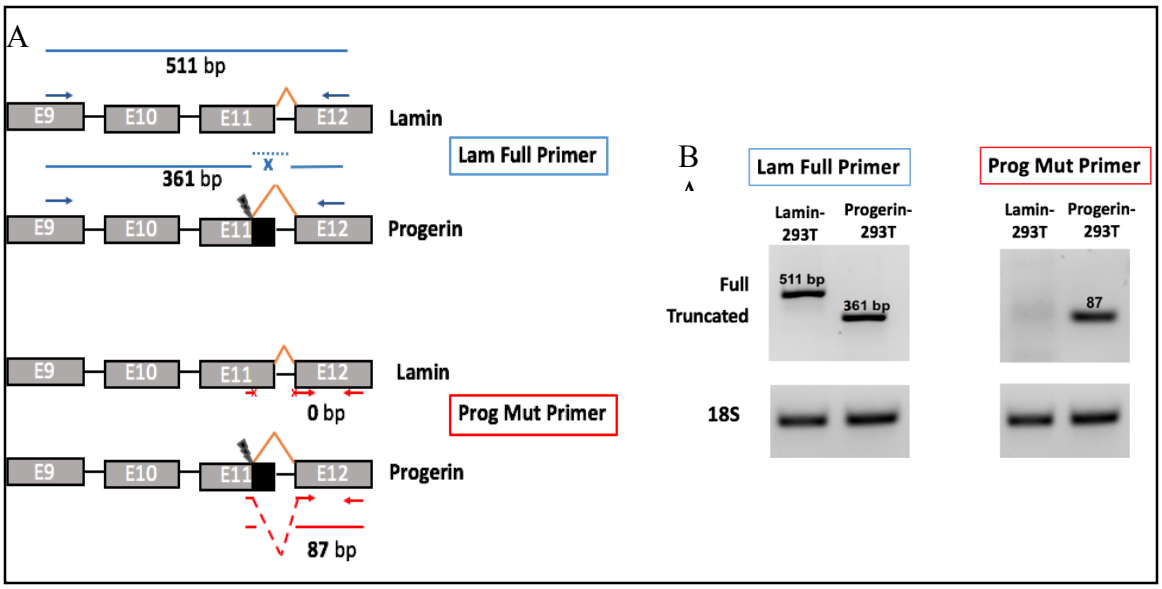

Figure 3-2: Truncated lamin expression in progerin transfected HEK293Ts

(**A**) Primer pairs designed to verify the expression of full length (wildtype) lamin and truncated (Mutant) progerin (adapted from Scaffidi, P. and Misteli, T., 2006). The lam full primer pair spans across exon 9 and 11 across the consensus splice sequence. In the lamin transfected cells, a 511 bp product is expected to be PCR amplified. In cells overexpressing progerin, a 150 bp deletion causes the expression of a truncated product of 361 bp. The prog mut primer pair detects parts of exon 11-12 that is discontinuous in wild type lamin, but yields an 87 bp product in progerin overexpressing cells.

(**B**) The overexpression of full length Lamin/truncated progerin in infected HEK293Ts was confirmed by qRT-PCR using primer pairs designed in (a). The products were run on a 4% agarose gel to enhance band resolution.

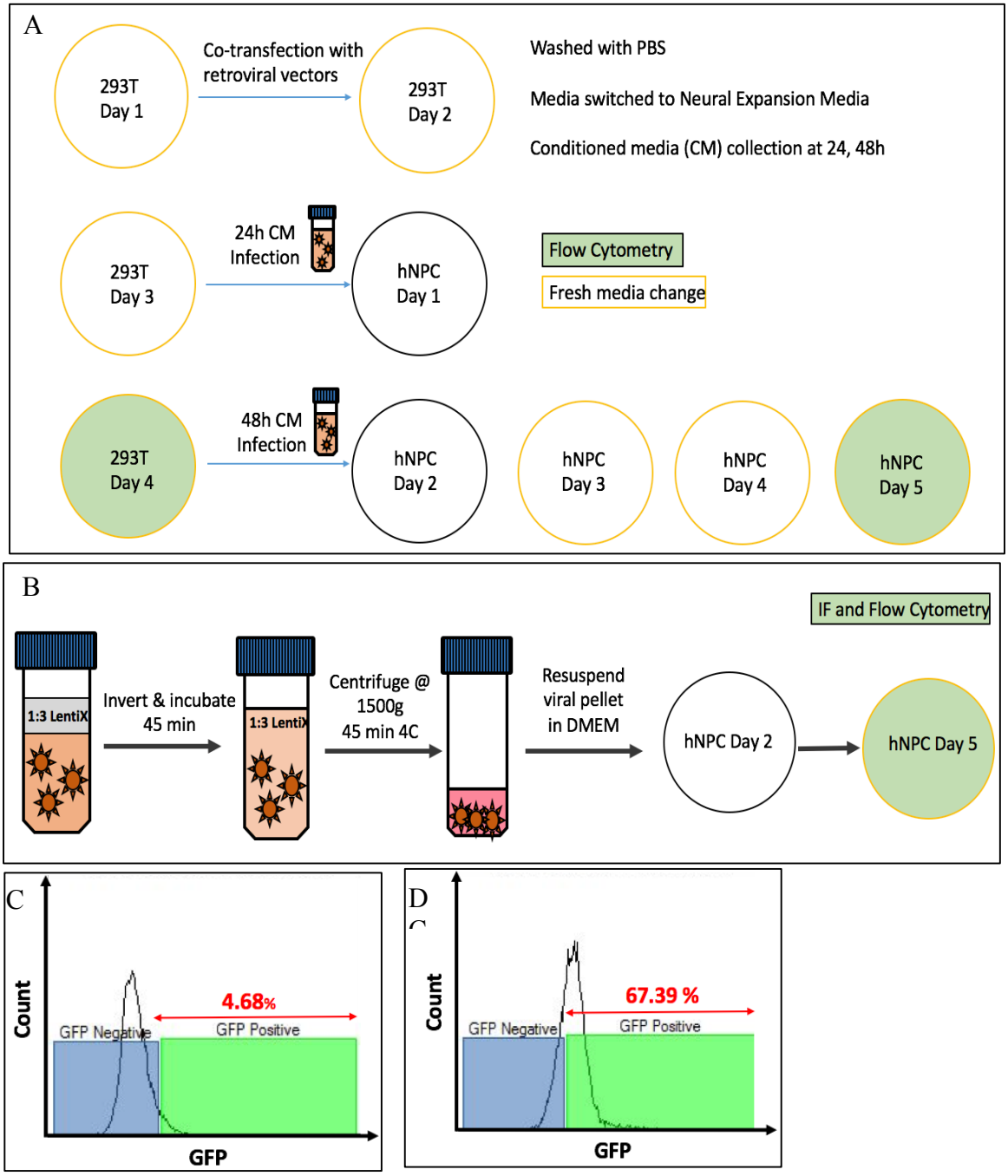

Figure 3-3 Chemical concentration increases transduction efficiency

(A)Transduction of human neural progenitor cells (hNPCs) with viral conditioned neural expansion media. (B) LentiX mediated concentration of cell supernatant. Transduction efficiency using no concentration (C) and LentiX (D) was measured using flow cytometry.

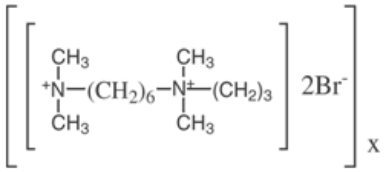

POLYBRENE

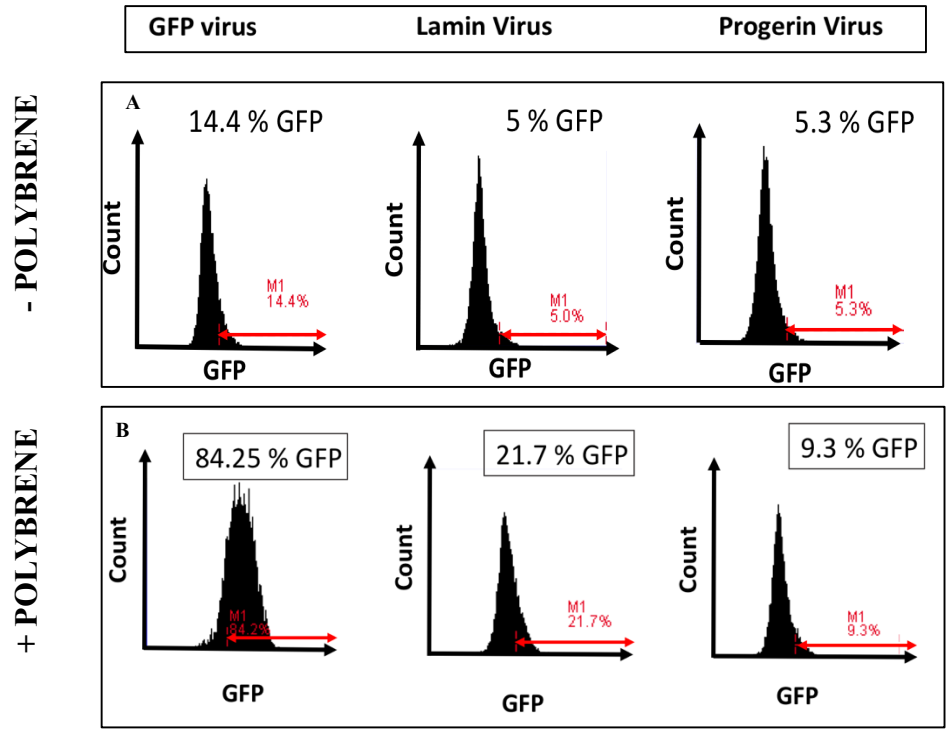

Figure 3-4 Transduction efficiency in the presence of polybrene

Flow cytometry data indicating GFP positive population of cells as a measure of transduction efficiency of GFP, Lam-GFP and Prog-GFP viruses. The transduction efficiency was higher in the presence of polybrene **(B)** for all three viruses, compared to the no treatment control **(A).**

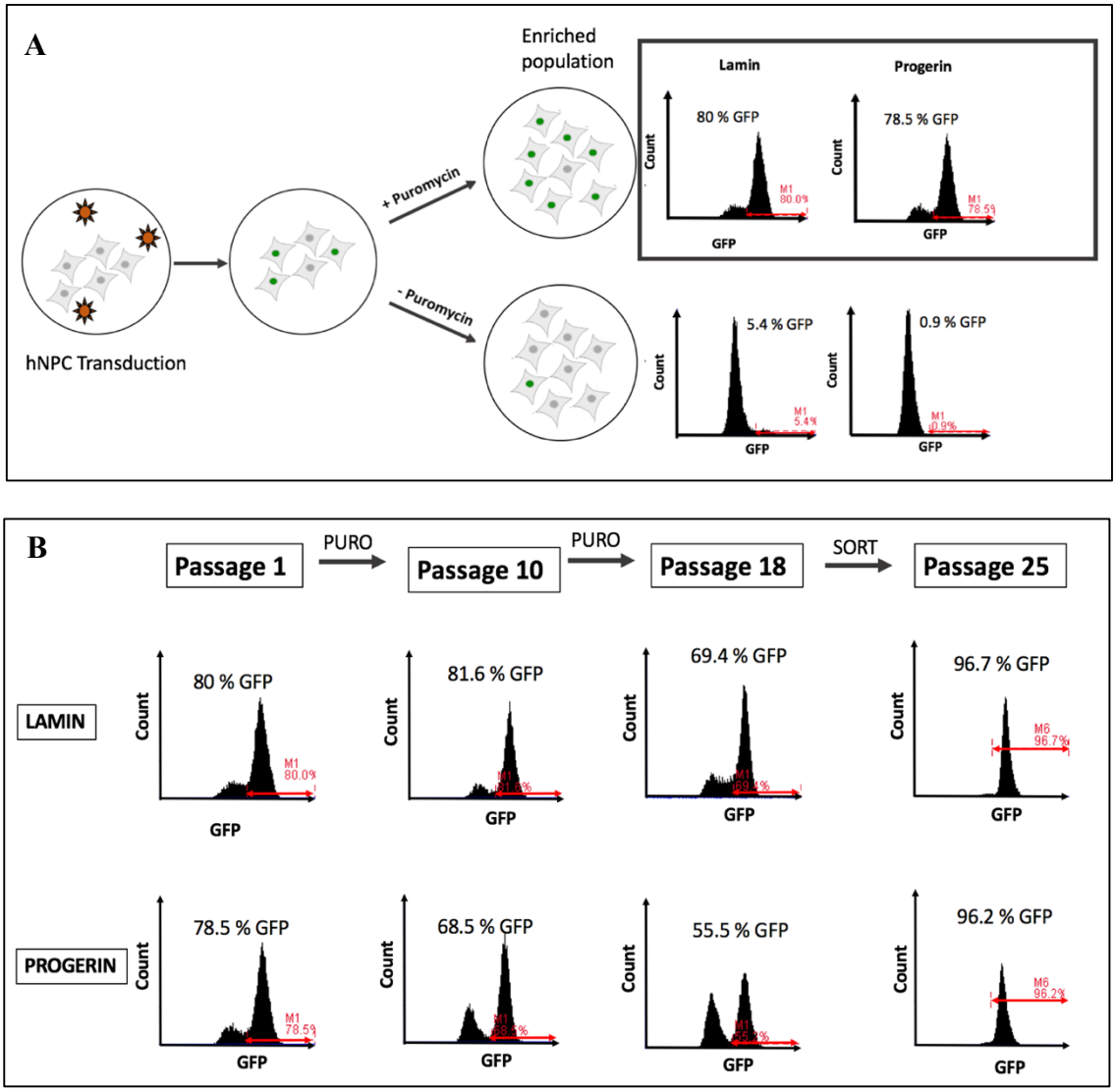

Figure 3-5 Puromycin selects pure population of transduced hNPCs

Flow cytometry data of Lam-GFP and Prog-GFP virus transduced hNPCs. Pure populations of GFP positive transduced cells were obtained using puromycin selection(**A**). Lamin/ progerin hNPC population was enriched at passage 25 by FACs (**B**).

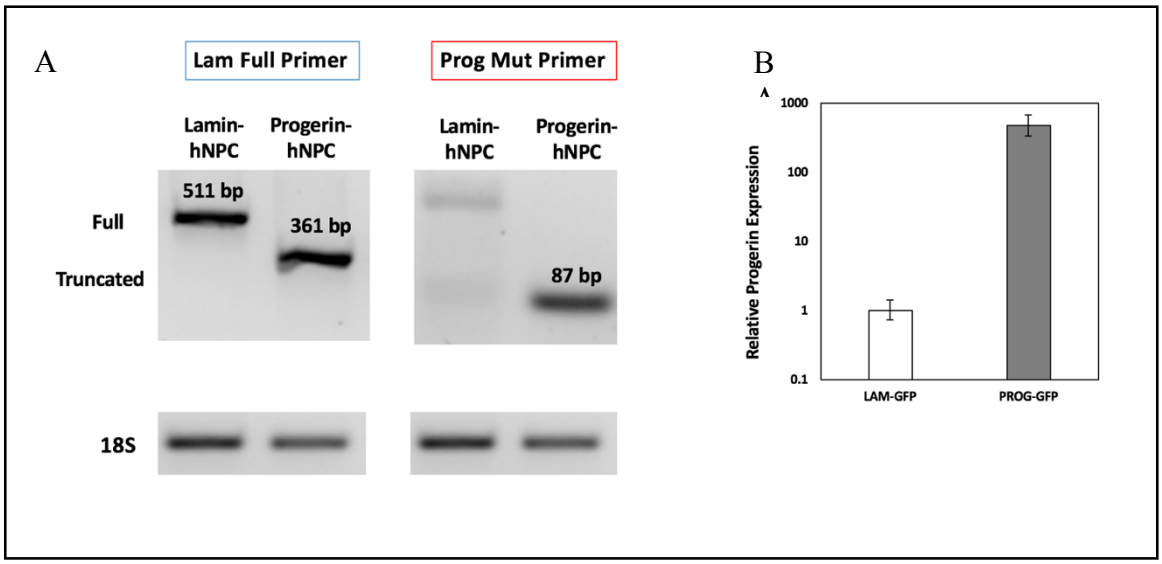

Figure 3-6 Truncated lamin overexpressed in Progerin-GFP hNPCs.

(A) 4% agarose gel with qRT-PCR products with primers designed to detect full length (511 bp) and truncated lamin (361 bp) (**Figure 3-2**) in lamin and progerin hNPCs using the 'lam full' primer pair. The expression of mutant progerin is confirmed by the presence of an 87 bp product with the 'prog mut' primer in Progerin-GFP transduced hNPCs.

(B) Relative progerin expression in progerin-GFP transduced cells was ~1000 fold higher compared to progerin levels in lamin-GFP hNPCs.

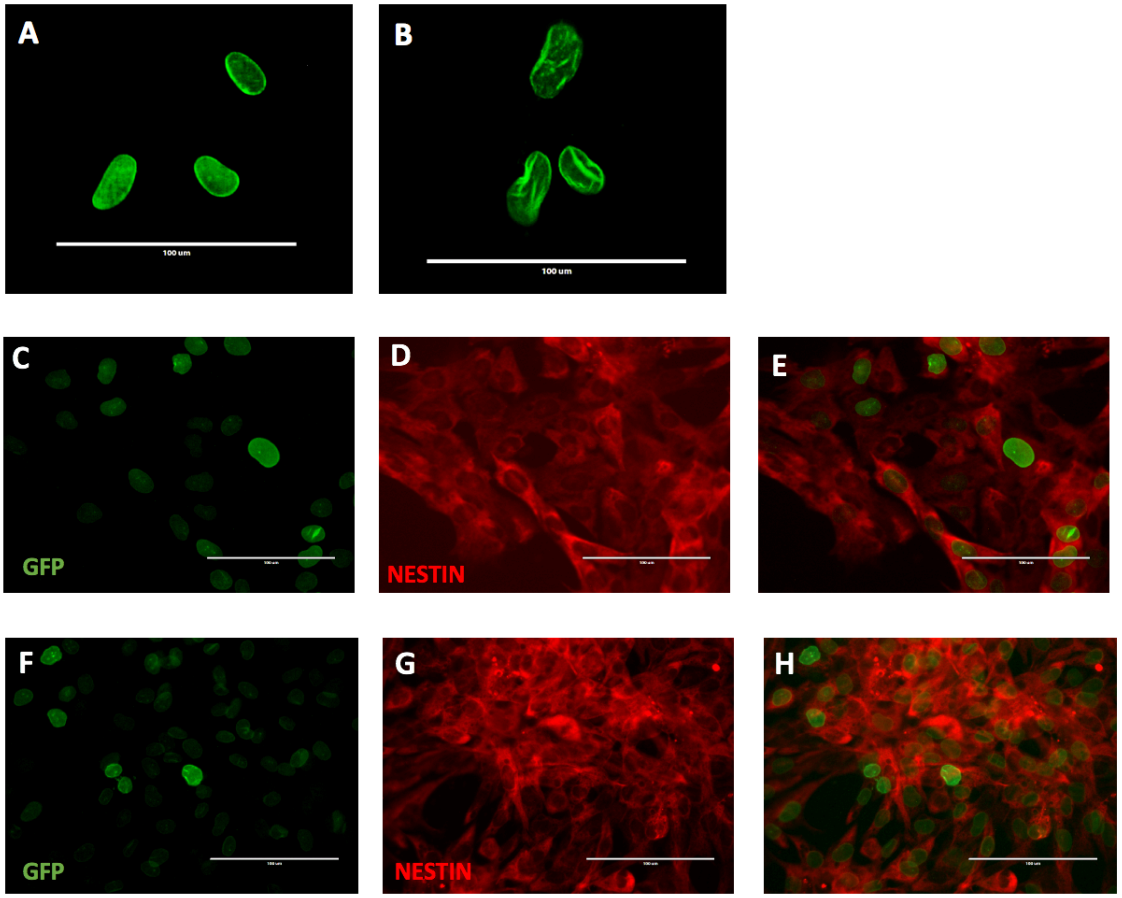

Figure 3-7 Progerin overexpression causes blebbing of nuclear envelope.

Epifluorescence microscopy images of wild type lamin-GFP (**A**) and progerin-GFP (**B**) transduced hNPC nuclei. The Progerin-GFP nuclear envelope. (scale=100um). Immunofluorescence images of NESTIN stained lamin(**C-E**)/progerin(**F-H**) hNPCs.

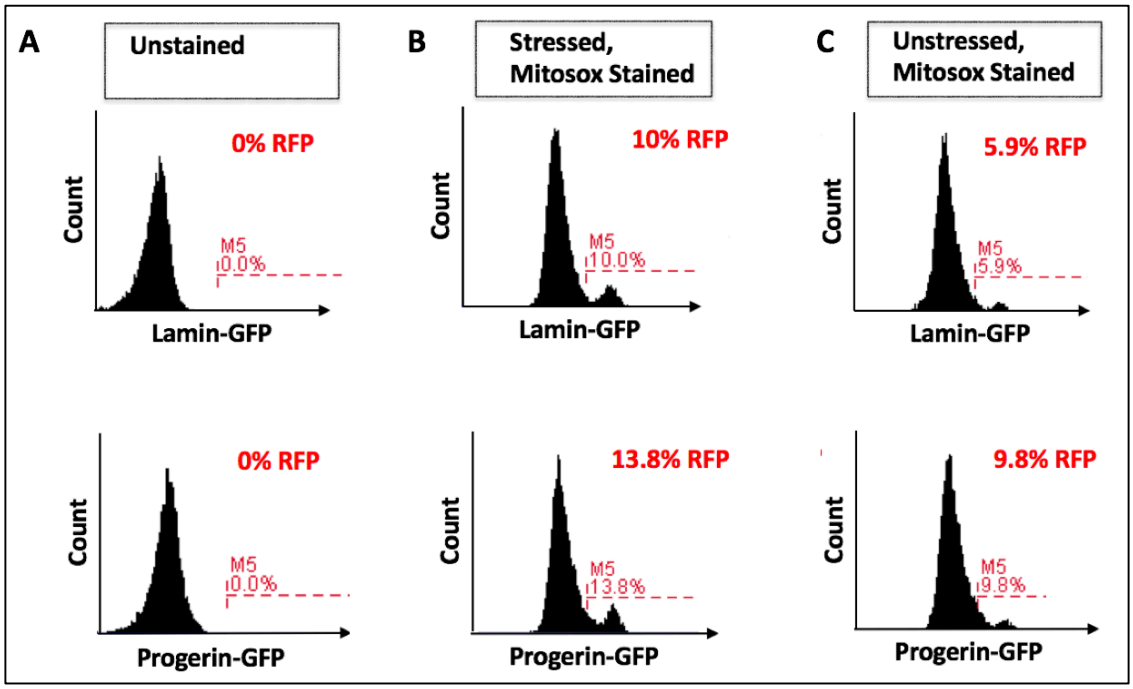

Figure 3-8 Progerin overexpression in hNPCs leads to elevated mitochondrial ROS. Flow cytometry analysis of Lamin/Progerin-GFP hNPCs to quantify mitochondrial reactive oxidation species (ROS). Carbonyl cyanide 3-chlorophenylhydrazone-induced stress was used to measure ROS in Lamin/Progerin-GFP hNPCs (**B**), with unstained hNPCs as the threshold for red fluorescent protein(RFP) signal. In the absence of the chemical stressor, Progerin-GFP hNPCs exhibit higher ROS levels than Lamin-GFP hNPCs (**C**).

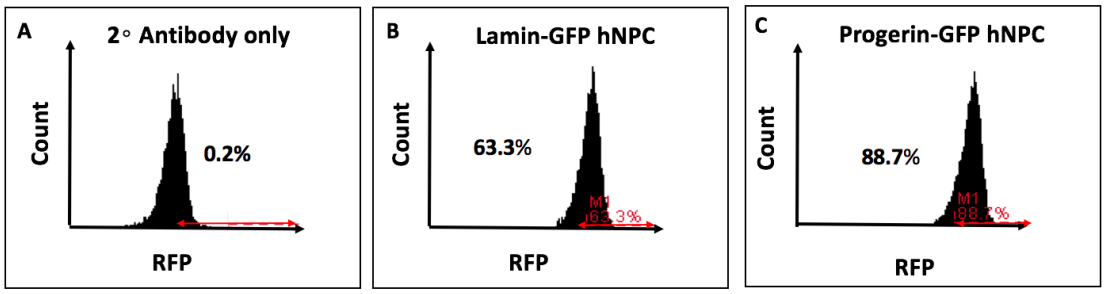

Figure 3-9 Progerin-GFP hNPCs display increased levels of repressive histone methylation marks

Flow cytometry analysis of cells immunostained for the repressive histone methylation mark H3K27me3. hNPCs stained with secondary antibody only was used to gate the RFP positive histone marks**(A)**. Progerin transduced hNPCs express high levels of the repressive epigenetic mark **(C)** compared to the Lamin-GFP cells **(B)**.

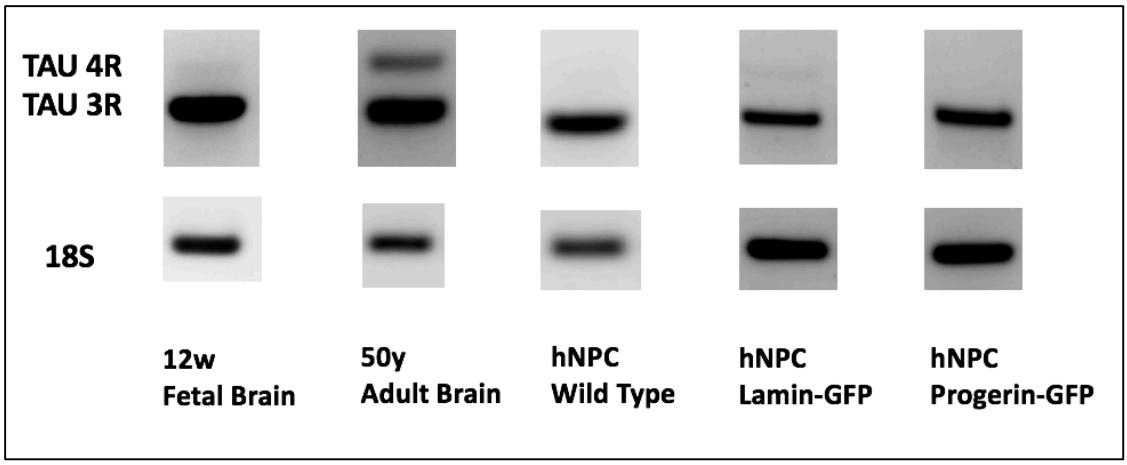

Figure 3-10 Tau 4R isoform not Expressed in transduced hNPCs

A 2% agarose gel containing the qRT-PCR products of fetal brain (12 weeks), adult brain (50-years), wt hNPCs, Lamin-GFP hNPCs and Progerin-GFP hNPCs for Tau gene expression. The 4R isoform is observed only in the adult brain sample, whereas all samples express the 3R Tau isoform.

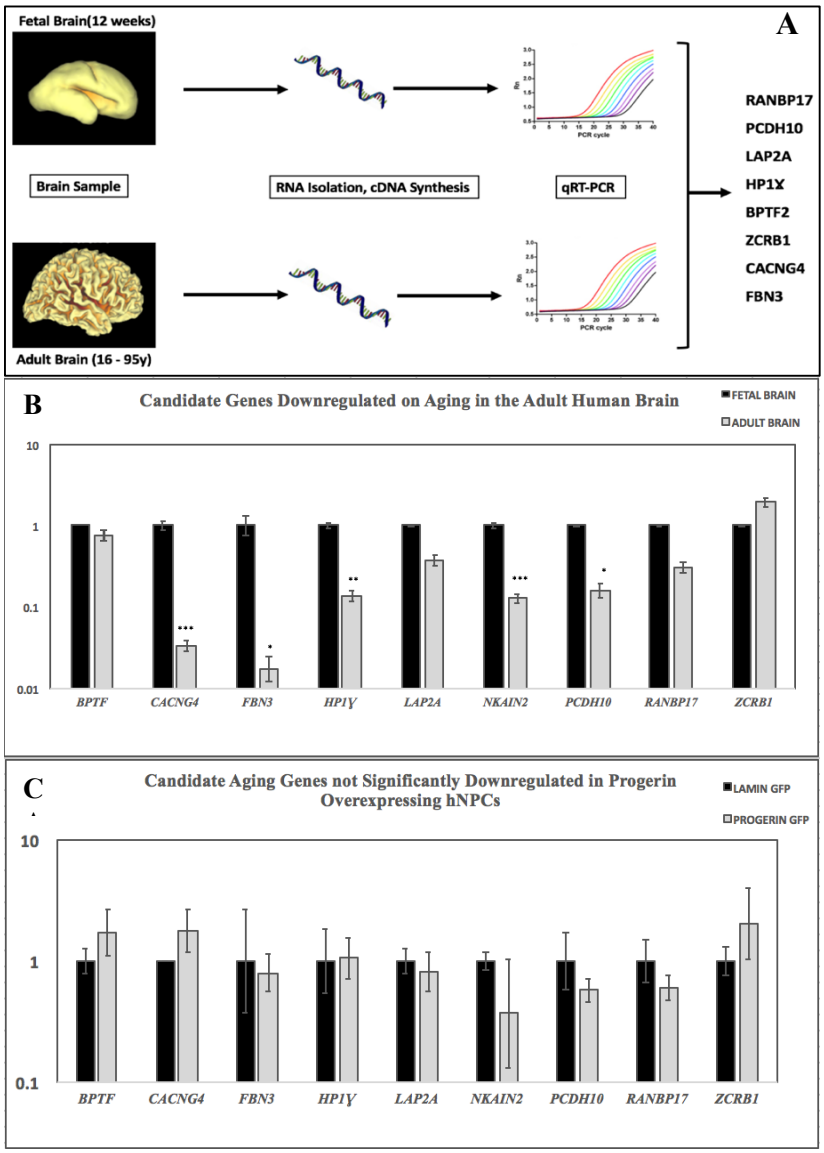

Figure 3-11 Progerin transduced hNPCs exhibit Lamin-GFP hNPC like expression levels of genes downregulated during aging. cDNA from fetal and adult brain tissue was used to measure age related gene expression levels of 9 genes **(A)**. The gene expression of 5 candidate aging genes was significantly reduced in the adult cortical brain samples compared to fetal brain gene expression levels ($p<0.05$) (**B**). The expression of aging genes in the Progerin-GFP hNPCs was not significantly different from Lamin-GFP hNPCs **(C)**. Comparisons were made using Students t-test ($p<0.05$, 0.001,0.0001)

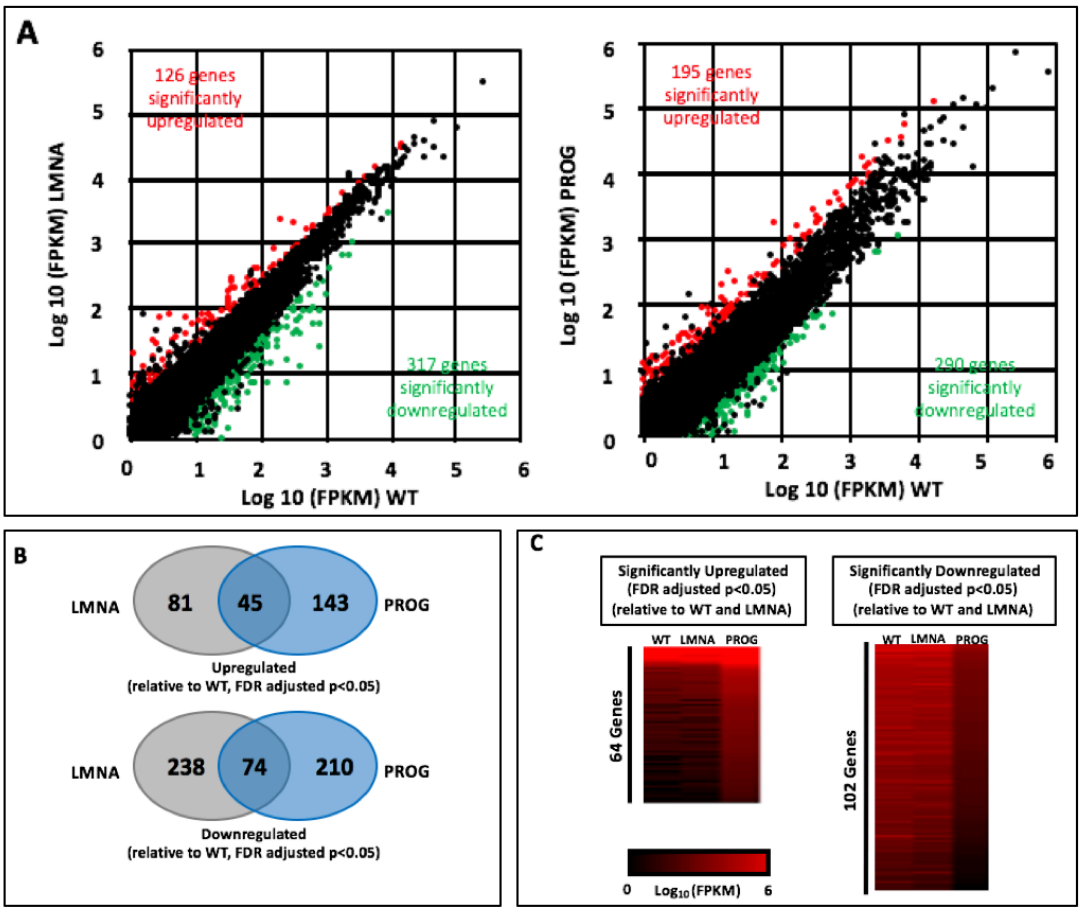

Figure 3-12 RNA-Seq analysis reveals the differential expression of Progerin hNPCs

RNA-Seq analysis of Lamin-GFP, Progerin-GFP and wt hNPCs. False discovery rate (FDR) adjusted differential gene expression of Lamin-GFP and Progerin-GFP transduced cells relative to the wild type hNPCs (**A**-**B**). Upregulation of gene expression on transgene overexpression is indicated in red and downregulation is indicated in green. The Progerin-GFP hNPCs show significant differential upregulation of 64 genes and downregulation of 102 genes compared to both the wild type and Lamin-GFP hNPCs (**C**).

4. DISCUSSION

The maturation, or aging, of patient derived hPSCs is required to recapitulate the functional phenotypes observed *in vivo*. Although DNA damage and chemical stressors can be used to induce some of the biochemical markers associated with aging, the study of disease mechanism in such a model could be biased due to these external stresses. The prolonged constitutive overexpression of the progerin protein in hNPCs could affect the AD phenotype itself. This problem can be addressed with the development of a lentiviral system to inducibly express the progerin protein. This method would allow us to control the extent of overexpression of progerin and in turn, the age of the cell. The induction of the aged phenotype could also be achieved by introducing the progerin point mutation in the consensus splice-site of endogenous *LMNA* gene using CRISPR technology.

In our study, we established a retroviral system to stably integrate the mutant *LMNA* gene, associated with accelerated aging in HGPS, into the genome of hNPCs. The constitutive expression of the mutant progerin protein at the progenitor stem cell stage was observed to induce some hallmarks of aging such as the blebbing of the nuclear envelope, elevated mitochondrial ROS, and high levels of the repressive H3K27me3 histone mark. The terminal differentiation of these progerin expressing hNPCs into cell types of the central nervous system could lead to the manifestation of the other age related phenotypes, including the expression of the 4R Tau isoform and the downregulation of nuclear transport proteins. The genes implicated in aging (RANBP17, LAP2A etc.) were downregulated in cortical neurons and the directed differentiation of hNPCs to this specific population is expected to recapitulate this phenotype. Additionally, these cells could recapitulate functional phenotypes missing in current models using both healthy and AD.

REFERENCES

BECKER, A. J., MC, C. E. & TILL, J. E. 1963. Cytological demonstration of the clonal nature of spleen colonies derived from transplanted mouse marrow cells. *Nature,* 197**,** 452-4.

BRAFMAN, D. A. 2015. Generation, Expansion, and Differentiation of Human Pluripotent Stem Cell (hPSC) Derived Neural Progenitor Cells (NPCs). *Methods Mol Biol,* 1212**,** 87-102.

BROOKMEYER, R., EVANS, D. A., HEBERT, L., LANGA, K. M., HEERINGA, S. G., PLASSMAN, B. L. & KUKULL, W. A. 2011. National estimates of the prevalence of Alzheimer's disease in the United States. *Alzheimers Dement,* 7**,** 61-73.

BROOKMEYER, R., KAWAS, C. H., ABDALLAH, N., PAGANINI-HILL, A., KIM, R. C. & CORRADA, M. M. 2016. Impact of interventions to reduce Alzheimer's disease pathology on the prevalence of dementia in the oldest-old. *Alzheimers Dement,* 12**,** 225-32.

CAPELL, B. C., COLLINS, F. S. & NABEL, E. G. 2007. Mechanisms of cardiovascular disease in accelerated aging syndromes. *Circ Res,* 101**,** 13-26.

COFFIN, J. M. 1992. Genetic diversity and evolution of retroviruses. *Curr Top Microbiol Immunol,* 176**,** 143-64.

DAVIS, H. E., MORGAN, J. R. & YARMUSH, M. L. 2002. Polybrene increases retrovirus gene transfer efficiency by enhancing receptor-independent virus adsorption on target cell membranes. *Biophys Chem,* 97**,** 159-72.

DENNING, W., DAS, S., GUO, S., XU, J., KAPPES, J. C. & HEL, Z. 2013. Optimization of the transductional efficiency of lentiviral vectors: effect of sera and polycations. *Mol Biotechnol,* 53**,** 308-14.

ERIKSSON, M., BROWN, W. T., GORDON, L. B., GLYNN, M. W., SINGER, J., SCOTT, L., ERDOS, M. R., ROBBINS, C. M., MOSES, T. Y., BERGLUND, P., DUTRA, A., PAK, E., DURKIN, S., CSOKA, A. B., BOEHNKE, M., GLOVER, T. W. & COLLINS, F. S. 2003. Recurrent de novo point mutations in lamin A cause Hutchinson-Gilford progeria syndrome. *Nature,* 423**,** 293-8.

FANALES-BELASIO, E., RAIMONDO, M., SULIGOI, B. AND BUTTÒ, S., 2010. HIV virology and pathogenetic mechanisms of infection: a brief overview. *Annali dell'Istituto superiore di sanita*, *46*(1), pp.5-14.

GOATE, A., CHARTIER-HARLIN, M. C., MULLAN, M., BROWN, J., CRAWFORD, F., FIDANI, L., GIUFFRA, L., HAYNES, A., IRVING, N., JAMES, L.

& ET AL. 1991. Segregation of a missense mutation in the amyloid precursor protein gene with familial Alzheimer's disease. *Nature,* 349**,** 704-6.

IOVINO, M., PATANI, R., WATTS, C., CHANDRAN, S. & SPILLANTINI, M. G. 2010. Human stem cell-derived neurons: a system to study human tau function and dysfunction. *PLoS One,* 5**,** e13947.

JAMES, B. D., LEURGANS, S. E., HEBERT, L. E., SCHERR, P. A., YAFFE, K. & BENNETT, D. A. 2014. Contribution of Alzheimer disease to mortality in the United States. *Neurology,* 82**,** 1045-50.
KIM, J., BASAK, J. M. & HOLTZMAN, D. M. 2009. The role of apolipoprotein E in Alzheimer's disease. *Neuron,* 63**,** 287-303.

LAPASSET, L., MILHAVET, O., PRIEUR, A., BESNARD, E., BABLED, A., AIT-HAMOU, N., LESCHIK, J., PELLESTOR, F., RAMIREZ, J. M., DE VOS, J., LEHMANN, S. & LEMAITRE, J. M. 2011. Rejuvenating senescent and centenarian human cells by reprogramming through the pluripotent state. *Genes Dev,* 25**,** 2248-53.

LIU, C. C., KANEKIYO, T., XU, H. & BU, G. 2013. Apolipoprotein E and Alzheimer disease: risk, mechanisms and therapy. *Nat Rev Neurol,* 9**,** 106-18.

LOUIS, N., EVELEGH, C. & GRAHAM, F. L. 1997. Cloning and sequencing of the cellular-viral junctions from the human adenovirus type 5 transformed 293 cell line. *Virology,* 233**,** 423-9.

MARION, R. M., STRATI, K., LI, H., TEJERA, A., SCHOEFTNER, S., ORTEGA, S., SERRANO, M. & BLASCO, M. A. 2009. Telomeres acquire embryonic stem cell characteristics in induced pluripotent stem cells. *Cell Stem Cell,* 4**,** 141-54.

MERTENS, J., PAQUOLA, A. C., KU, M., HATCH, E., BOHNKE, L., LADJEVARDI, S., MCGRATH, S., CAMPBELL, B., LEE, H., HERDY, J. R., GONCALVES, J. T., TODA, T., KIM, Y., WINKLER, J., YAO, J., HETZER, M. W. & GAGE, F. H. 2015. Directly Reprogrammed Human Neurons Retain Aging-Associated Transcriptomic Signatures and Reveal Age-Related Nucleocytoplasmic Defects. *Cell Stem Cell,* 17**,** 705-18.

MERTENS, J., PAQUOLA, A. C., KU, M., HATCH, E., BOHNKE, L., LADJEVARDI, S., MCGRATH, S., CAMPBELL, B., LEE, H., HERDY, J. R., GONCALVES, J. T., TODA, T., KIM, Y., WINKLER, J., YAO, J., HETZER, M. W. & GAGE, F. H. 2015. Directly Reprogrammed Human Neurons Retain Aging-Associated Transcriptomic Signatures and Reveal Age-Related Nucleocytoplasmic Defects. *Cell Stem Cell,* 17**,** 705-18.

MILLER, J. D., GANAT, Y. M., KISHINEVSKY, S., BOWMAN, R. L., LIU, B., TU, E. Y., MANDAL, P. K., VERA, E., SHIM, J. W., KRIKS, S., TALDONE, T., FUSAKI, N., TOMISHIMA, M. J., KRAINC, D., MILNER, T. A., ROSSI, D. J. & STUDER, L. 2013. Human iPSC-based modeling of late-onset disease via progerin-induced aging. *Cell Stem Cell,* 13**,** 691-705.

MOYA, N., CUTTS, J., GAASTERLAND, T., WILLERT, K. & BRAFMAN, D. A. 2014. Endogenous WNT signaling regulates hPSC-derived neural progenitor cell heterogeneity and specifies their regional identity. *Stem Cell Reports,* 3**,** 1015-28.

NAYEROSSADAT, N., MAEDEH, T. & ALI, P. A. 2012. Viral and nonviral delivery systems for gene delivery. *Adv Biomed Res,* 1**,** 27.

ODDO, S., CACCAMO, A., SHEPHERD, J. D., MURPHY, M. P., GOLDE, T. E., KAYED, R., METHERATE, R., MATTSON, M. P., AKBARI, Y. & LAFERLA, F. M. 2003. Triple-transgenic model of Alzheimer's disease with plaques and tangles: intracellular Abeta and synaptic dysfunction. *Neuron,* 39**,** 409-21.

PIACERI, I., NACMIAS, B. & SORBI, S. 2013. Genetics of familial and sporadic Alzheimer's disease. *Front Biosci (Elite Ed),* 5**,** 167-77.

PRIGIONE, A., HOSSINI, A. M., LICHTNER, B., SERIN, A., FAULER, B., MEGGES, M., LURZ, R., LEHRACH, H., MAKRANTONAKI, E., ZOUBOULIS, C. C. & ADJAYE, J. 2011. Mitochondrial-associated cell death mechanisms are reset to an embryonic-like state in aged donor-derived iPS cells harboring chromosomal aberrations. *PLoS One,* 6**,** e27352.

SCAFFIDI, P. & MISTELI, T. 2005. Reversal of the cellular phenotype in the premature aging disease Hutchinson-Gilford progeria syndrome. *Nat Med,* 11**,** 440-5.

SCAFFIDI, P. & MISTELI, T. 2006. Lamin A-dependent nuclear defects in human aging. *Science,* 312**,** 1059-63.

SHERRINGTON, R., FROELICH, S., SORBI, S., CAMPION, D., CHI, H., ROGAEVA, E. A., LEVESQUE, G., ROGAEV, E. I., LIN, C., LIANG, Y., IKEDA, M., MAR, L., BRICE, A., AGID, Y., PERCY, M. E., CLERGET-DARPOUX, F., PIACENTINI, S., MARCON, G., NACMIAS, B., AMADUCCI, L., FREBOURG, T., LANNFELT, L., ROMMENS, J. M. & ST GEORGE-HYSLOP, P. H. 1996. Alzheimer's disease associated with mutations in presenilin 2 is rare and variably penetrant. *Hum Mol Genet,* 5**,** 985-8.

SHERRINGTON, R., ROGAEV, E. I., LIANG, Y., ROGAEVA, E. A., LEVESQUE, G., IKEDA, M., CHI, H., LIN, C., LI, G., HOLMAN, K., TSUDA, T., MAR, L., FONCIN, J. F., BRUNI, A. C., MONTESI, FRASER, P. E., ROMMENS, J. M. & ST

GEORGE-HYSLOP, P. H. 1995. Cloning of a gene bearing missense mutations in early-onset familial Alzheimer's disease. *Nature,* 375**,** 754-60.

SOLDNER, F. & JAENISCH, R. 2012. Medicine. iPSC disease modeling. *Science,* 338**,** 1155-6.

ST GEORGE-HYSLOP, P. H., TANZI, R. E., POLINSKY, R. J., HAINES, J. L., NEE, L., WATKINS, P. C., MYERS, R. H., FELDMAN, R. G., POLLEN, D., DRACHMAN, D. & ET AL. 1987. The genetic defect causing familial Alzheimer's disease maps on chromosome 21. *Science,* 235**,** 885-90.

ST GEORGE-HYSLOP, P., HAINES, J., ROGAEV, E., MORTILLA, M., L., POLLEN, D., POLINSKY, R., NEE, L., KENNEDY, J., MACCIARDI, F., ROGAEVA, E., LIANG, Y., ALEXANDROVA, N., LUKIW, W., SCHLUMPF, K., TANZI, R., TSUDA, T., FARRER, L., CANTU, J. M., DUARA, R., AMADUCCI, L., BERGAMINI, L., GUSELLA, J., ROSES, A., CRAPPER MCLACHLAN, D. & ET AL. 1992. Genetic evidence for a novel familial Alzheimer's disease locus on chromosome 14. *Nat Genet,* 2**,** 330-4.

SUZUKI, S., NAMIKI, J., SHIBATA, S., MASTUZAKI, Y. & OKANO, H. 2010. The neural stem/progenitor cell marker nestin is expressed in proliferative endothelial cells, but not in mature vasculature. *J Histochem Cytochem,* 58**,** 721-30.

TAKAHASHI, K., TANABE, K., OHNUKI, M., NARITA, M., ICHISAKA, T., TOMODA, K. & YAMANAKA, S. 2007. Induction of pluripotent stem cells from adult human fibroblasts by defined factors. *Cell,* 131**,** 861-72.

TANG, Y., LI, T., LI, J., YANG, J., LIU, H., ZHANG, X. J. & LE, W. 2014. Jmjd3 is essential for the epigenetic modulation of microglia phenotypes in the immune pathogenesis of Parkinson's disease. *Cell Death Differ,* 21**,** 369-80.

TISCORNIA, G., SINGER, O. & VERMA, I. M. 2006. Production and purification of lentiviral vectors. *Nat Protoc,* 1**,** 241-5.

VANGUILDER, H. D., VRANA, K. E. & FREEMAN, W. M. 2008. Twenty-five years of quantitative PCR for gene expression analysis. *Biotechniques,* 44**,** 619-26.

VICKERS, J. C., MITEW, S., WOODHOUSE, A., FERNANDEZ-MARTOS, C. M., KIRKCALDIE, M. T., CANTY, A. J., MCCORMACK, G. H. & KING, A. E. 2016. Defining the earliest pathological changes of Alzheimer's disease. *Curr Alzheimer Res,* 13**,** 281-7.

VIDAK, S., KUBBEN, N., DECHAT, T. & FOISNER, R. 2015. Proliferation of progeria cells is enhanced by lamina-associated polypeptide 2alpha (LAP2alpha) through expression of extracellular matrix proteins. *Genes Dev,* 29**,** 2022-36.

WEINBERG, J. B., MATTHEWS, T. J., CULLEN, B. R. & MALIM, M. H. 1991. Productive human immunodeficiency virus type 1 (HIV-1) infection of nonproliferating human monocytes. *J Exp Med,* 174**,** 1477-82.

WEUVE, J., HEBERT, L. E., SCHERR, P. A. & EVANS, D. A. 2014. Deaths in the United States among persons with Alzheimer's disease (2010-2050). *Alzheimers Dement,* 10**,** e40-6.

YANG, F., UEDA, K., CHEN, P., ASHE, K. H. & COLE, G. M. 2000. Plaque-associated alpha-synuclein (NACP) pathology in aged transgenic mice expressing amyloid precursor protein. *Brain Res,* 853**,** 381-3.

ZUFFEREY, R., DULL, T., MANDEL, R. J., BUKOVSKY, A., QUIROZ, D., NALDINI, L. & TRONO, D. 1998. Self-inactivating lentivirus vector for safe and efficient in vivo gene delivery. *J Virol,* 72**,** 9873-80.

APPENDIX A

TABLE 1: PRIMARY BRAIN SAMPLES USED FOR GENE EXPRESSION ANALYSIS

	Sample	Source	Age
1	Fetal Brain		0
2	Miami_004	University of Miami Brain Endowment Bank	16
3	Miami_008	University of Miami Brain Endowment Bank	22
4	13152	University of Pittsburg	23
5	13095	University of Pittsburg	33
6	09-35 CBL	Banner Sun Health Research Institute	38
7	13054	University of Pittsburg	48
8	13068	University of Pittsburg	48
9	13058	University of Pittsburg	50
10	13032	University of Pittsburg	52
11	09-50 CBL	Banner Sun Health Research Institute	53
12	13052	University of Pittsburg	66
13	Miami_009	University of Miami Brain Endowment Bank	70
14	10-70 CBL	Banner Sun Health Research Institute	74
15	13-49 CBL	Banner Sun Health Research Institute	75
16	Miami_001	University of Miami Brain Endowment Bank	79
17	Miami_025	University of Miami Brain Endowment Bank	87
18	10-39 CBL	Banner Sun Health Research Institute	93
19	10-26 CBL	Banner Sun Health Research Institute	95

APPENDIX B

TABLE 2: PRIMER PAIRS USED IN RT-QPCR

	Primer Name	Primer sequence
1	LMNA-RT9 FWD(Full/Trunc)	GTGGAAGGCACAGAACACCT
2	LMNA-RT12 RVS(Full/Trunc)	GTGAGGAGGACGCAGGAA
3	LMNA Δ150 exon12 FWD	GCGTCAGGAGCCCTGAGC
4	LMNA Δ150 exon12 RVS	GACGCAGGAAGCCTCCAC
5	LMNA-RTnorm e8 Forward	GGTGGTGACGATCTGGGCT
6	LMNA-Rtnorm e9 Reverse	CCAGTGGAGTTGATGAGAGC
7	qRanBP17#1 FWD	GGATCCTGGATTGAGACGAA
8	qRanBP17#1 REV	GTGCTTCCAGGCTCGTTCTA
9	qRanBP17#2 FWD	CACTGAACCATGCAGTCTCG
10	qRanBP17#2 REV	GGGCTAGCCAACATCACTGT
11	qRanBP17#3 FWD	TCTGAATTACGTGGCATCACA
12	qRanBP17#3 REV	CCTCAAACCACCCCAACTTA
15	PCDH10 #1 FWD	CCTGGCATGGACTCTGTTCC
16	PCDH10 #1 REV	TAGCTGCCTCCACAATAGCTT
17	PCDH10 #2 FWD	GTTCCTGGCATGGACTCTGT
18	PCDH10 #2 REV	AGCTGCCTCCACAATAGCTTC
19	LAP2α FWD	TCCTTTGGGCAGTACCGAAC
20	LAP2α RVS	AGACCAACATGGCACTGTG
21	HP1Gamma-2 FWD	AGACTCCGGTCACTGTCCTC
22	HP1Gamma-2 RVS	ACTTGAAGAGCTATTACGTTCGC
23	18S FWD	GTAACCCGTTGAACCCCATT
24	18S RVS	CCATCCAATCGGTAGTAGCG
25	TAU FWD	AAGTCGCCGTCTTCCGCCAAG
26	TAU RVS	GTCCAGGGACCCAATCTTCGA
27	CACNG4-3 FWD	CCAACCTGACCATGGACGAC
28	CACNG4-3 RVS	TAGATCCCTTCGATGCAGCAC
29	ZCRB1-2 FWD	GCTACGAAGAGTCGGGGTTG
30	ZCRB1-2 RVS	CCACCACTCATTTCTTCAGGT
31	FBN3-1 FWD	GACTGACCCGGACAACTGAG
32	FBN3-1 RVS	AGAAGGGAGAGACCCCTGTC
33	BPTF-2 FWD	CAAATCGGAGAAGTCCAACGG
34	BPTF-2 RVS	CCAGTACCTCTTTGCCCTCC
35	NKAIN2-2 FWD	GGGCACCTATCCTGGCAAAT
36	NKAIN2-2 RVS	TCAGGATAAGGTCTGTTTCCTTTGA

APPENDIX C

VECTOR MAP OF PROGERIN VIRAL CONSTRUCT

Progerin Viral Vector

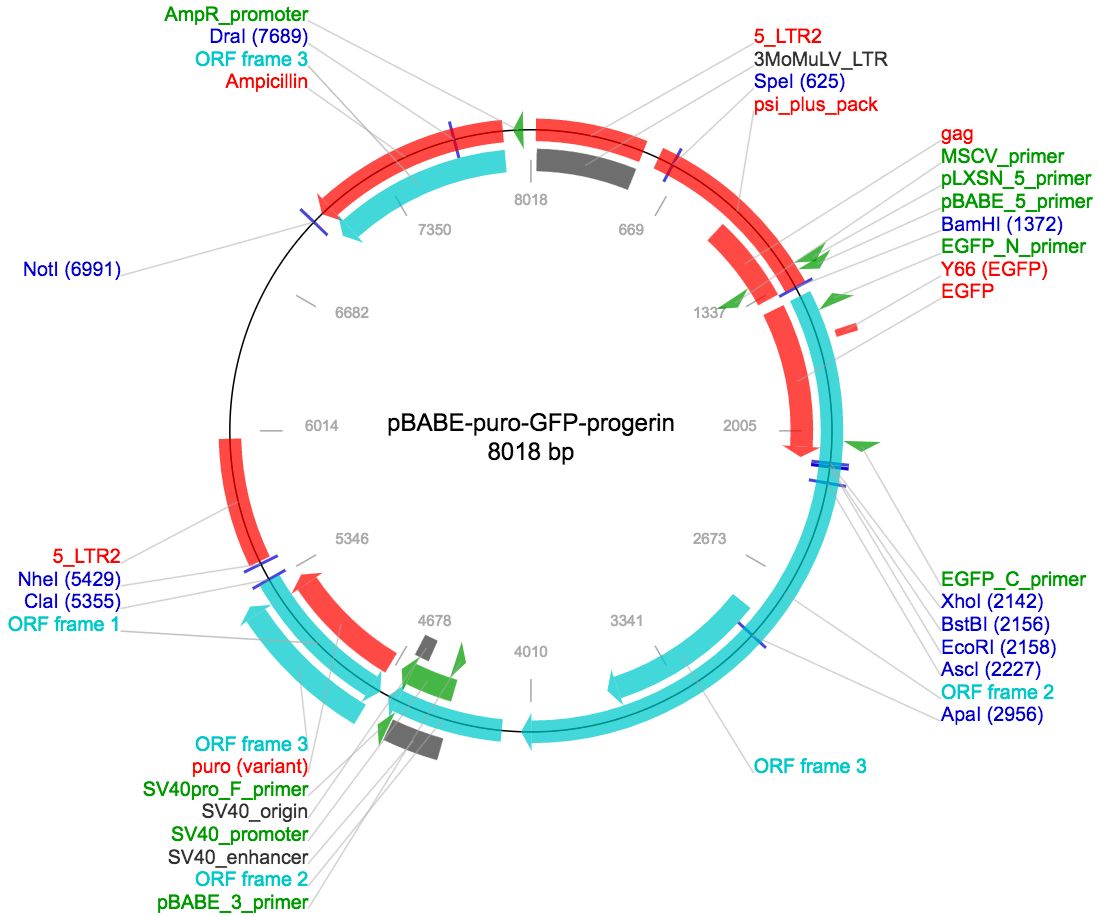

(Addgene #17663)

Lamin Viral Vector

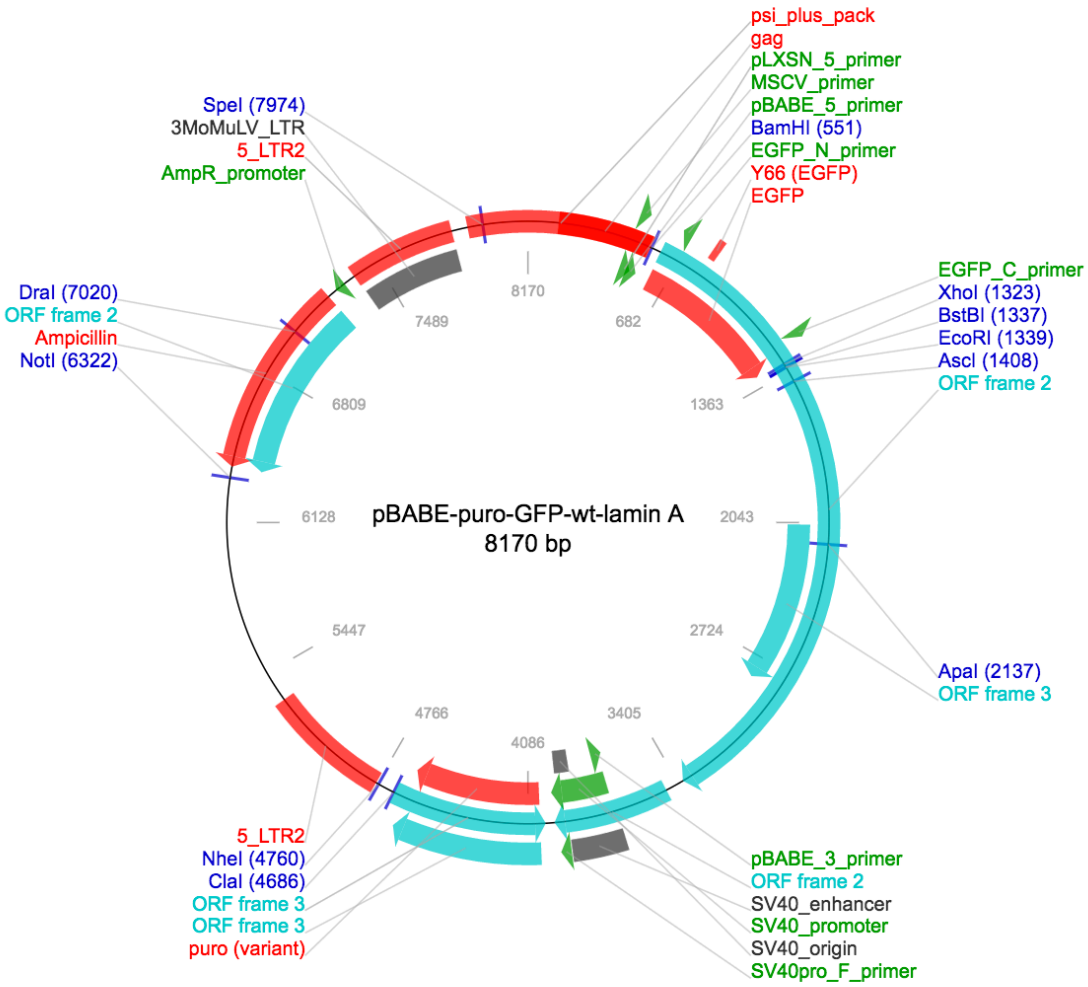

(Addgene # 17662)